ISTANBUL TECHNICAL UNIVERSITY ★ GRADUATE SCHOOL

INVESTIGATION OF THE EFFECT OF C-MYC TRANSCRIPTION FACTOR ON TRANSCRIPTIONAL REGULATION OF *ATP13A2* GENE

M.Sc. THESIS

Aslı Beril TİRYAKİLER

Department of Molecular Biology-Genetics and Biotechnology

Molecular Biology-Genetics and Biotechnology Programme

DECEMBER 2023

ISTANBUL TECHNICAL UNIVERSITY ★ GRADUATE SCHOOL

INVESTIGATION OF THE EFFECT OF C-MYC TRANSCRIPTION FACTOR ON TRANSCRIPTIONAL REGULATION OF *ATP13A2* GENE

M.Sc. THESIS

Aslı Beril TİRYAKİLER
(521201103)

Department of Molecular Biology-Genetics and Biotechnology

Molecular Biology-Genetics and Biotechnology Programme

Thesis Advisor: Prof. Dr. Arzu Karabay

DECEMBER 2023

İSTANBUL TEKNİK ÜNİVERSİTESİ ★ LİSANSÜSTÜ EĞİTİM ENSTİTÜSÜ

ATP13A2 GENİNİN TRANSKRİPSİYONEL REGÜLASYONUNDA C-MYC TRANSKRİPSİYON FAKTÖRÜNÜN ETKİSİNİN İNCELENMESİ

YÜKSEK LİSANS TEZİ

Aslı Beril TİRYAKİLER
(521201103)

Moleküler Biyoloji-Genetik ve Biyoteknoloji Anabilim Dalı

Moleküler Biyoloji-Genetik ve Biyoteknoloji Programı

Tez Danışmanı: Prof. Dr. Arzu Karabay

ARALIK 2023

Aslı Beril TİRYAKILER, a M.Sc student of ITU Graduate School student ID 521201103, successfully defended the thesis/dissertation entitled "Investigation of the Effect of c-myc Transcription Factor on Transcriptional Regulation of *ATP13A2* Gene", which she prepared after fulfilling the requirements specified in the associated legislations, before the jury whose signatures are below.

Thesis Advisor:	**Prof. Dr. Arzu KARABAY** Istanbul Technical University	....
Jury Members:	**Prof. Dr. Ayça Sayı Yazgan** Istanbul Technical University	....
	Prof. Dr. Meral Yüksel Marmara University	....

Date of Submission : 4 July 2023
Date of Defense : 25 September 2023

To my beautiful family, my best friends and my dear boyfriend,

FOREWORD

I'd like to thank Prof. Dr. Arzu KARABAY for giving me this opportunity to study under her supervision. Her support and guidance throughout my research have been incredibly valuable.

I would like to thank my thesis committee members Prof. Dr. Ayça Sayı YAZGAN and Prof. Dr. Meral YÜKSEL for devoting their precious time to listen and critique my presentation. Your comments and criticisms hold incredible value in my heart.

Also, I want to thank to my dearest lab mates Ezgi ERTEREK, Ezgi SELÇUK, Benan TEMİZCİ, Ece SELÇUK ŞAHİN, Seren KÜÇÜKVARDAR, Ilgın IŞILTAN, Şeyma AKARSU and Dr. Koray KIRIMTAY for their support for the past 3 years. I have learned so much from you and I will forever cherish the memories I have created with you here.

I also need to thank to my best friends Öykü ELASLAN, Mısra ÖZKURT, Ege SERBAN, and Gökberk DEMİREZ for always being by my side and holding my hand.

I owe a special thanks to my beloved family; my mom, Işıl YENİDOĞAN DAĞ and my dad, Hasan DAĞ for their infinite support. I wouldn't be able to do anything without you standing right behind me to support me whenever I stumble, and my sister Bilge Nehir TİRYAKİLER for always giving a hug when I need one.

And finally, I'd like to thank my amazing boyfriend Berkant OLÇAY for always believing in me, even when I did not believe in myself.

September 2023 Aslı Beril TİRYAKİLER

TABLE OF CONTENTS

Page

ABBREVIATIONS

µg : Microgram
µl : Microliter
µM : Micromolar
Ab : Antibody
BSA : Bovine Serum Albumin
DNA : Deoxyribonucleic Acid
dNTP : Deoxyribonucleotide
EDTA : Ethylenediaminetetraacetic acid
DMEM : Dulbecco's Modified Eagle Medium
DMSO : Dimethyl sulfoxide
FBS : Fetal Bovine Serum
g : Gram
Ig : Immunoglobulin
KRS : Kufor Rakep Syndrome
mg : Milligram
ml : Milliliter
mM : Millimolar
mRNA : Messenger RNA
ng : Nanogram
nm : Nanometer
nM : Nanomolar
NMD : Non-sense mediated decay
PBS : Phosphate Buffered Saline
PCR : Polymerase Chain Reaction
RNA : Ribonucleic Acid
RT : Room temperature
RT-PCR : Real time Polymerase Chain Reaction

LIST OF TABLES

LIST OF FIGURES

Page

INVESTIGATION OF THE EFFECT OF C-MYC TRANSCRIPTION FACTOR ON TRANSCRIPTIONAL REGULATION OF ATP13A2 GENE

SUMMARY

A rare neurodegenerative disease diagnosed as Kufor Rakeb Syndrome (KRS) is also known as an atypical early-onset form of Parkinson's disease (PD). KRS is characterized by symptoms of spasticity, dementia, and supranuclear gaze palsy in addition to other symptoms of PD. KRS has been linked with mutations that occur in *ATP13A2* (*PARK9*) gene. *ATP13A2 gene*, expresses the ATP13A2 protein which is known to have a role in the transport of inorganic cations through the membrane of the cell. ATP13A2 belongs to the P5 type ATPase transporter protein family and it can predominantly be found in lysosomes. ATP13A2 protects the cellular homeostasis of metal cations such as Fe3+, Zn2+, Mn2+, and Ca2+, and increases the degradation of accumulated alpha-synuclein, and even maintains the function of organelles including lysosome, mitochondria and endoplasmic reticulum.

Previous research carried out in our laboratory discovered that a frameshift mutation forming a pre-termination codon (PTC) in the *ATP13A2* gene leads to the degradation of ATP13A2 mRNA through the non-sense-mediated decay (NMD) mechanism, which in turn leads to an inhibition of the expression of the ATP13A2 protein in patients' fibroblasts. During a previous study done in our laboratory, it was found that when the NMD suppressor drug known as 5-azacytidine was administered to patient cells as well as healthy control cells, a significant increase in the level of ATP13A2 mRNA was observed in control fibroblasts as well as patient fibroblasts.

These results could be explained by several different mechanisms. According to the findings of a previous study, the NMD pathway can be inhibited by the c-Myc transcription factor. In addition, c-Myc is thought to have a role in the NMD inhibitory mechanism of 5-azacytidine. When 5-azacytidine was administered to the cells, it was detected that c-Myc protein expression level was increased compared to the control group. Our earlier research showed that 5-azacytidine not only stops NMD from working in patient fibroblasts, but also raises the amount of ATP13A2 mRNA in control fibroblasts. This could be due to 5-azacytidine causing an increase in the amount of c-Myc transcription factor. In order to regulate the expression of *ATP13A2*, the c-Myc transcription factor can directly access the CACGTG (E-Box) regions that are located in the *ATP13A2* promoter by forming a heterodimer with its potential binding partners such as Max (MYC-Associated Factor X) protein.

The *c-Myc* (*MYC*) gene expresses a transcription factor that can bind to the DNA and it is capable of both activating and inhibiting transcription. c-Myc targets many different genes that are involved with the essential cellular functions. Some examples for this could be cell proliferation division and cell cycle progression. c-Myc is also essential for DNA replication. The c-Myc transcription factor can heterodimerize with Max to regulate gene expression. It has been proposed that c-Myc functions as a master regulator of global genome expression, and in this capacity Myc regulates essential

cellular functions. The dysregulation of c-Myc expression has been linked to the development of several fatal diseases, including cancer, due to its wide array of target genes. Therefore, a comprehensive study of the genomic targets of c-Myc is required for understanding the unexplained nature of this gene family's complex biological functions and to develop novel therapeutic strategies.

For these reasons, the effects of the c-Myc transcription factor on ATP13A2 protein and mRNA expression were investigated during this study. Firstly, the binding sites of c-Myc were detected using bioinformatic tools. In order to detect the binding sites of c-Myc on the 2000 bp *ATP13A2* promoter site in vivo, ChIP assay was performed. Western blot experiments have shown that when the c-Myc transcription factor is overexpressed in HEK293T cells, the amount of ATP13A2 protein expression increases; however, the luciferase reporter assay and qRT-PCR results revealed that the mRNA levels of ATP13A2 decreased 48 hours after c-Myc overexpression. When qRT-PCR and western blot experiments were done in a time dependent manner, a significant increase was observed at 7^{th} and 8^{th} hours followed by a significant decrease at 48^{th} hour.

The findings of this experiment suggest that ATP13A2 may activate a feedback mechanism to reduce mRNA and protein levels closer to their normal level, following the significant increase in protein and mRNA levels first observed 7 and 8 hours after c-Myc overexpression. The initial increase in the ATP13A2 mRNA and protein levels of the c-Myc transcription factor at the 8th hour turns into a significant decrease at the 48th hour.

In addition, our findings indicate that the c-Myc transcription factor has an impact on the levels of ATP13A2 protein expression however there are certainly other transcription factors that could also be affecting the overall expression levels of ATP13A2 protein levels due to c-Myc affecting global gene expression. One example to such transcription factor could be HIF1A which is known to upregulate ATP13A2 expression. To determine if HIF1A could be responsible from the increase in ATP13A2 protein, HIF1A expression levels were targeted for further investigation. Western blot and qPCR experiments showed that upon c-Myc overexpression, HIF1A protein and mRNA levels were increased compared to control groups.

Finally, when c-Myc transcription factor was overexpressed in patient fibroblasts by nucleofection, NMD inhibition in patient fibroblasts was observed, which made it possible for the truncated protein that is the result of a frameshift mutation in the *ATP13A2* gene to be seen at approximately 50 kDa in western blot analysis.

ATP13A2 GENİNİN TRANSKRİPSİYONEL REGÜLASYONUNDA C-MYC TRANSKRİPSİYON FAKTÖRÜNÜN ETKİSİNİN İNCELENMESİ

ÖZET

Parkinson hastalığının (PH) atipik erken başlangıçlı formu olarak da bilinen Kufor-Rakeb Sendromu (KRS) olarak teşhis edilen nadir bir nörodejeneratif hastalık olan KRS, PH'nın semptomları yanı sıra spastisite, demans ve supranükleer bakış felci semptomları ile karakterizedir. KRS'nin, ATP13A2 (PARK9) olarak bilinen transmembran proteininde meydana gelen genetik bir mutasyonun sonucu ortaya çıktığı belirlenmiştir. P5 ATPaz taşıyıcı ailesinin bir üyesi olan ATP13A2, ağırlıklı olarak lizozomlarda bulunmaktadır. Araştırmaya göre ATP13A2, Fe3+, Mn2+, Zn2+ ve Ca2+ gibi metal katyonlarının hücre içerisindeki homeostazını korumakla birlikte, fazla alfa-sinüklein ve poliaminlerin eliminasyonunu arttırmakta ve aynı zamanda lizozom, endoplasmik retikulum ve mitokondri gibi organellerin işlevini sürdürmelerini sağlamaktadır. *ATP13A2* (*PARK9*) geni, inorganik katyonların hücre zarından taşınmasını sağlayan çok geçişli membran proteini olan ATP13A2'nin kodlanmasını sağlar ve hücre içi inorganik katyonların taşınması görevini yapan *ATP13A2* genindeki mutasyonlar, KRS hastalığı ile ilişkilendirilmiştir.

Laboratuvarımızda gerçekleştirilen önceki araştırma sırasında, *ATP13A2* genindeki ön sonlandırma kodonu (PTC) oluşturan bir çerçeve kayması mutasyonunun, hastaların fibroblastlarında ATP13A2 mRNA'nın anlamsız aracılı mRNA bozulması (NMD) mekanizması yoluyla degredasyona yol açtığı keşfedilmiştir. Bu durum çerçeve kayması, mutasyonuna sahip hasta fibroblastlarında güdük ATP13A2 proteininin ekspresyonunun inhibisyonuna yol açmaktadır. 5-azasitidin olarak bilinen NMD baskılayıcı ilaç bu çerçeve kaymasına sahip olan hasta fibroblastlarına uygulandığında, güdük ATP13A2 proteininin ekspresyonu gözlenmiştir fakat hasta fibroblastlarının yanı sıra, 5-azasitidin ilacı sağlıklı kontrol hücrelerine uygulandığında, hasta fibroblastlarında gözlemlenen ATP13A2 mRNA artışının yanı sıra kontrol fibroblastlarında da ATP13A2 mRNA seviyesinde önemli bir artış gözlemlenmesine yol açmıştır.

Bu elde edilen sonuçlar birkaç farklı mekanizma ile açıklanabilir. Önceki bir çalışmanın bulguları, NMD mekanizmasının, c-Myc transkripsiyon faktörü tarafından inhibe edilebilir olduğunu göstermiştir. Ek olarak, c-Myc'nin 5-azasitidin ilacının inhibe edici mekanizmasında etkili bir rolü olduğu düşünülmektedir. Laboratuvarımızda yapılan araştırmalarda, hücrelere 5-azasitidin uygulandığında, c-Myc protein ekspresyon düzeylerinin kontrol grubuna göre arttığı saptanmıştır. Daha önceki araştırmamızda, 5-azasitidin'in yalnızca NMD mekanizmasının hasta fibroblastlarında çalışmasını durdurmakla kalmayıp, aynı zamanda kontrol fibroblastlarında ATP13A2 mRNA miktarını da arttırdığını göstermiştir.

Bunun nedeni, c-Myc transkripsiyon faktörü miktarında bir artışa neden olan 5-azasitidin ilacının etkisi olabilir. ATP13A2'nin ekspresyonunu düzenlemek için, c-Myc transkripsiyon faktörü, potansiyel bağlanma partnerleri ile heterodimer

oluşturarak *ATP13A2* promotorunda bulunan CACGTG (E-Box) bölgelerine doğrudan erişebilir ve ekspresyon seviyesini düzenleyebilir. Max (MYC-Associated Factor X) proteini bu potansiyel bağlanma partnerlerinden birine örnek olarak verilebilir.

c-myc (*MYC*), hem genleri aktive edebilen hem de inhibe edebilen bir transkripsiyon faktörünü kodlar. c-Myc, bu mekanizma aracılığıyla hücre proliferasyonu ve hücre döngüsü ilerlemesi gibi temel hücresel fonksiyonları kontrol eden çok sayıda hedef genin ekspresyonunu düzenleyebilir. c-Myc, DNA replikasyonu için bile gereklidir. C-Myc, gen ekspresyonunu düzenlemek için Max ile heterodimerize olarak DNA'da E-box'lara bağlanır.

Max, transkripsiyonu ve c-Myc'yi inhibe etmek için Mad ailesi proteinleri ile heterodimerize olur. Myc'nin küresel genom ifadesinin ana düzenleyicisi olarak işlev gördüğü ve bu kapasitede Myc'nin temel hücresel işlevleri düzenlediği öne sürülmüştür. Myc ekspresyonunun düzensizliği, geniş hedef gen dizisi nedeniyle kanser de dahil olmak üzere birçok ölümcül hastalığın gelişimi ile ilişkilendirilmiştir. Bu nedenle, bu gen ailesinin karmaşık biyolojik işlevlerinin açıklanamayan doğasını anlamak ve yeni tedavi stratejiler geliştirmek için Myc'nin genomik hedeflerinin kapsamlı bir şekilde araştırılması gerekmektedir.

Bu nedenlerle bu çalışma sırasında c-Myc transkripsiyon faktörünün ATP13A2 proteini ve mRNA ekspresyonu üzerindeki etkilerinin belirlenmesi amaçlanmıştır. İlk olarak, biyoinformatik araçlar kullanılarak *ATP13A2* promotor bölgesinde, c-Myc'nin potansiyel bağlanma bölgeleri tespit edilmiştir. 2000 bp *ATP13A2* promotor bölgesindeki c-Myc transkripsiyon bağlanmasını in vivo olarak tespit etmek amacıyla ChIP analizi yapılmıştır. Western blot deneyleri, c-Myc transkripsiyon faktörünün HEK293T hücrelerinde aşırı eksprese edilmesi durumunda ATP13A2 protein ekspresyon miktarının arttığını; ancak lusiferaz raportör tahlili ve qRT-PCR sonuçları, ATP13A2'nin mRNA seviyelerinin c-Myc aşırı ekspresyonundan 48 saat sonra azaldığını ortaya çıkarmıştır. qRT-PCR ve western blot deneyleri zamana bağlı olarak yapıldığında 7. ve 8. saatlerde anlamlı bir artış, 48. saatte ise anlamlı bir düşüş gözlenmiştir.

Bu deneyin bulguları, ATP13A2'nin, protein ve mRNA seviyelerindeki ilk olarak 7-8. saatlerde gözlemlenen anlamlı artışın ardından, mRNA ve protein seviyelerini normal seviyesine yaklaştırarak azaltmak amacıyla bir geri bildirim mekanizmasını aktive edebileceğini göstermektedir. c-Myc transkripsiyon faktörünün ATP13A2 mRNA ve protein seviyesinde 8. saatte gerçekleştirdiği ilk artış, 48. saatte anlamlı bir azalışa dönüşmektedir.

Ek olarak, bulgularımız c-Myc transkripsiyon faktörünün ATP13A2 protein ekspresyonu seviyeleri üzerinde önemli bir etkiye sahip olduğunu göstermektedir, ancak c-Myc'nin global gen ekspresyonunu etkilemesi nedeniyle ATP13A2 protein ekspresyon seviyelerini dolaylı yoldan etkileyen başka mekanizmalar da kesinlikle var olmalıdır. Bu tür bir transkripsiyon faktörüne bir örnek, ATP13A2 ifadesini arttırdığı bilinen HIF1A transkripsiyon faktörü olabilir. ATP13A2 proteinindeki artıştan HIF1A'nın sorumlu olup olmadığını belirlemek için, c-Myc'e bağlı HIF1A ekspresyon seviyelerindeki değişimin araştırılması hedeflemiştir. Western blot ve qPCR deneyleri, c-Myc aşırı ekspresyonu üzerine HIF1A proteini ve mRNA seviyelerinin kontrol gruplarına kıyasla arttığını göstermektedir.

Son olarak, c-Myc transkripsiyon faktörü hasta fibroblastlarında nükleofeksiyon yoluyla aşırı eksprese edildiğinde, hasta fibroblastlarında NMD inhibisyonu gözlenmiş ve bu durum *ATP13A2* genindeki çerçeve kayması mutasyonu sonucu oluşan kısa proteinin western blot analizinde yaklaşık 50 kDa'da görülmesini mümkün kılmıştır.

1. INTRODUCTION

1.1 ATP13A2 (PARK9)

The *ATP13A2* gene has a total of 29 exons, which together code for a protein that is 1180 amino acids long. ATP13A2, which belongs to the family of P5-type ATPases, is a multi-pass transmembrane protein that contains 10 different transmembrane areas throughout its structure. It consists of three distinct functional sections that are denoted by their domain names: the ATPase and Nucleotide binding region which is denoted as the N-domain, the catalytic phosphorylation region which is denoted as P-domain, and the Actuator region which is named as the A-domain (Figure 1.1).

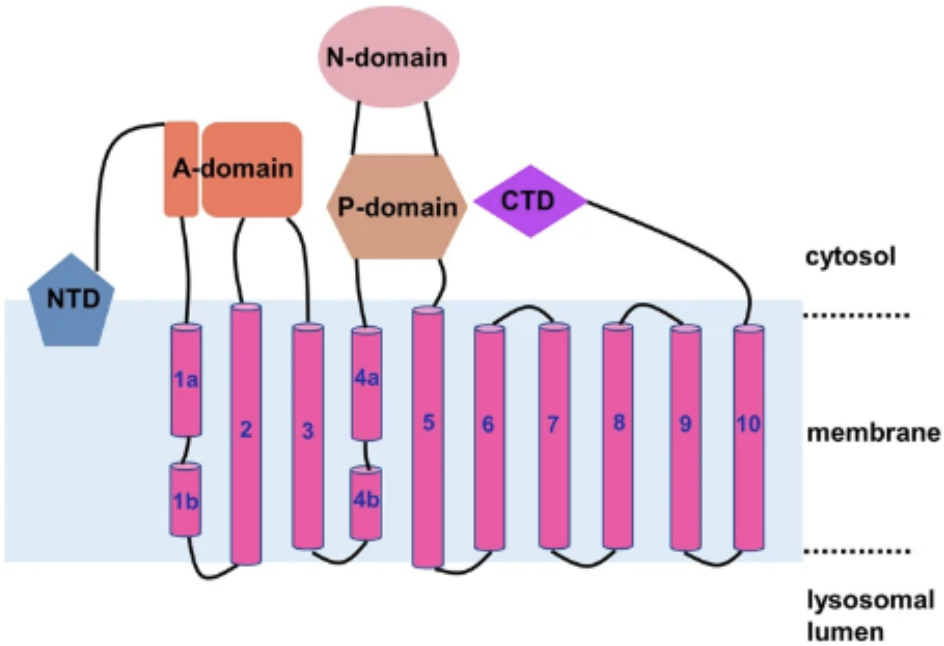

Figure 1.1: Representation of the ATP13A2 protein structure including the transmembrane domains (Chen et al., 2021).

The exact cellular function of these P5-type ATPases are not fully understood. What is known about them is that they require the usage of ATP in order to transport their specific substrate. Exact substrates of these ATPases are not well understood.

ATP13A2 protein can be found in late endosomes and lysosomes. It is being recognized as an important regulator of lysosomal processes. Mutations occurring on the *ATP13A2* gene have been linked to several different neurological conditions, such as Kufor-Rakeb syndrome (KRS) and Spastic Paraplegia-78 (SPG78) (Kong 2014). KRS is a severe, early-onset recessive form of Parkinson's disease that is associated with dementia. It is caused by mutations in the *ATP13A2* gene, which is part of the PARK9 Parkinson's disease susceptibility locus (Zhang et al. 2022). Mutations occurring in *ATP13A2* gene and how it causes a genetic disorder makes it clear that the ATP13A2 protein's function is crucial for the integrity of cellular mechanisms (Noch et al., 2017).

1.1.1 Pathogenic effects of ATP13A2 mutations

Mutations on the *ATP13A2* gene have been found to be associated with KRS, which is described as a rare variant of juvenile-onset atypical Parkinson disease that is associated with spasticity, supranuclear gaze palsy and dementia. There are several studies stating the effects of ATP13A2 on autophagy and mitochondrial clearance which could be relevant to the pathogenic effects of *ATP13A2* mutations. ATP13A2 expression is reported to be upregulated in response to oxidative stress which could be indicative as it's significant role in the clearance of cations that further contribute to the oxidative stress. ATP13A2 expression is also known to protect the cells from α-synuclein toxicity (van Veen et al. 2014). This could either be because of ATP13A2's ability to reduce the stress of accumulated α-synuclein, or ATP13A2 might be interfering with α-synuclein-membrane interactions. Mutated ATP13A2 proteins are thought to misfold and localize in the endoplasmic reticulum (ER) rather than the lysosome. Mislocalized proteins in the ER will be degraded by the ER degradation pathway, causing the ATP13A2 protein levels to decrease, particularly on the lysosome membrane. This decrease in ATP13A2 expression levels in patients can result in an impairment in autophagy since the decrease in ATP13A2, effects the lysosome's function to clear aggregated alpha-synuclein proteins (Zhang et al., 2022). Aggregated α-synuclein in Lewy bodies (LBs) is another important PD marker (Polymeropoulos et al., 1997). *SNCA* (α-synuclein) gene mutations were also linked to familial early-onset PD (Spillantini et al., 1997). α-synuclein overexpression causes ER stress, vesicle trafficking abnormalities, ubiquitin-proteasome system impairment, and mitochondrial dysfunction (Bendor et al., 2013).

ATP13A2 can also function as a lysosomal cation pump. In some of the KRS patients, iron accumulation is observed in patient's brain images. The excessive accumulation of iron has been identified as a contributing factor in the development and progression of PD. The substantia nigra is recognized as the principal brain area responsible for the deposition of iron, and it is within this region that the selective death of dopaminergic neurons takes place (Wang et al. 2016).

1.1.2 Kufor-Rakeb Syndrome

Dementia and Parkinsonism in early childhood characterize KRS which is an autosomal recessive illness occurs due to different loss-of-function mutations in *ATP13A2* (PARK9) gene (Yang et al., 2014). The symptoms occurring because of KRS syndrome are very similar to a regular PD however the most distinctive difference is that the initial symptoms of KRS develop at a much earlier age compared to PD. Overall, the rest of the symptoms of KRS can be ranged from slowness in the movement, tremors, ataxia and paraplegia.

The ATP13A2 protein can be expressed in a truncated form due to number of mutations, which causes loss-of-function (Park et al., 2011). Wild-type ATP13A2 protein is mostly found in late endosomal and lysosomal membranes, whereas the truncating KRS mutations cause the protein to stay in the ER, and this can cause ER stress and proteasomal breakdown through the ER-associated degradation pathway (Ramirez et al., 2006). ATP13A2 is essential for alpha-synuclein degradation via the lysosomal pathway, suggesting that in the case of a loss-of-function mutation, alpha-synuclein accumulation might be one of the physiological reasons of KRS symptoms. The study of PD patients' symptoms and genes revealed that the *ATP13A2* mutations have significant importance in the effects of PD. Gaining an accurate understanding of ATP13A2 and its mutations effects at the molecular level could get us one step closer to uncovering the complex mechanism of PD.

1.2 C-Myc as a Master Transcription Factor

The Myc oncogene is one of the most researched gene families in genomic research. c-Myc protein is a member of the basic helix-loop-helix-leucine zipper family of transcription factors. Myc modulates the dynamics of global gene expression through interactions with minor proteins such as Max, Mad/Mnt, Miz1. The oncogene c-Myc is known as a master transcription regulator that regulates numerous aspects of cellular processes (Figure 1.2). Since increased c-Myc expression positively affects cellular metabolims, it ends up changing the expression patern of many different proteins that are involved in cell division and proliferation within the cell. c-Myc increasing the metabolism and cell division rate can also increase the cell’s need of biological building blocks such as aminoacids, lipids and ions.

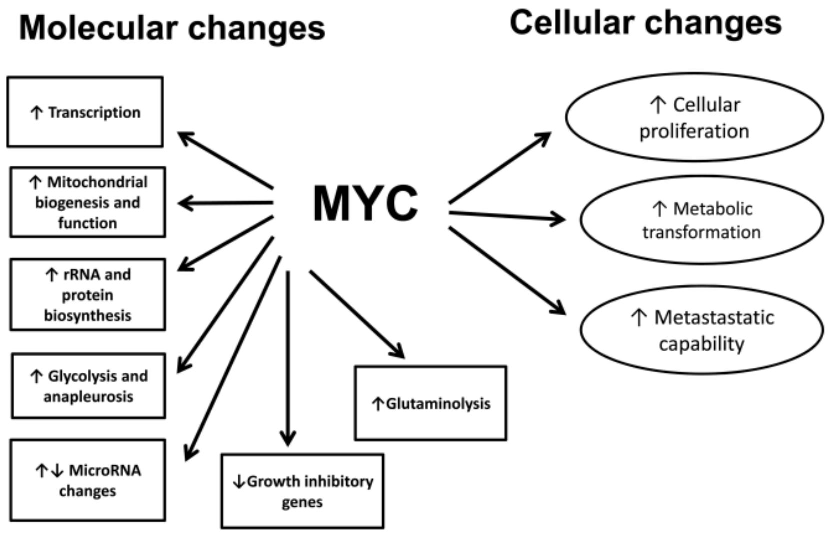

Figure 1.2: *MYC* gene effects many different cellular processes (Miller et al., 2012).

1.2.1 c-Myc binding sites and mechanisms

c-Myc recognizes E-box sequence which can be annotated as CANNTG, and it forms heterodimers with the Max transcription factor via their helix-loop-helix-leucine domains in order to bind to the E-boxes and increase gene expression (Chen et al., 2007). MAX transcription factor can also interact with MXD or MNT proteins in order to form repressor complexes (Figure 1.3). c-Myc dependent increased gene regulation, cell-cycle progression, apoptosis, and transformation depends on its interaction with MAX since c-Myc cannot form homodimers with itself (Mukherjee et al. 1992). Since the E-box sequence are relatively short and interchangeable, in theory c-Myc can bind to many different places in a promoter region. Non-specific binding of c-Myc and uncontrolled gene activation could be especially dangerous for the integrity and order within the cell since it could lead to different types of cancer. This is why c-Myc expression has to be tightly controlled within a healthy cell. Nonsense-mediated decay mechanism is essential for keeping the c-Myc mRNA levels low. Binding partners of c-Myc also help with stabilizing of actual needed c-Myc binding in a particular promoter binding region.

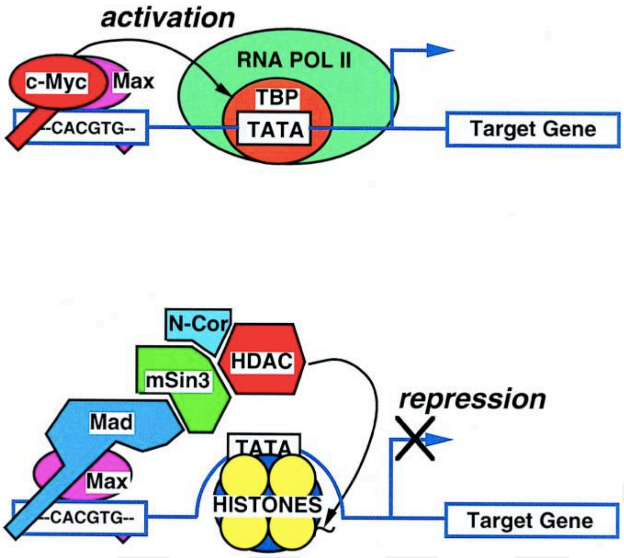

Figure 1.3: c-Myc/Max and Mad/Max heterodimers are shown with their effects on transcriptional regulation. The c-Myc/Max heterodimer can be seen attached to the E box 5′-CACGTG-3′ at the top (Dang et al., 2022).

1.3 Nonsense-Mediated mRNA Decay

Mutations are one of the fundamental forces of evolution, as they sustain population variability and thus facilitate evolutionary change. These mutations can be classified as advantageous or disadvantageous while many of these mutations will not show their effects. Certain mutations can create early stop codons which can cause translation process to terminate prematurely, causing truncated proteins. If premature termination codons are located further upstream from the exon-exon junction, mutations that generate these stop codons in mRNA can be sensed and degraded by the Nonsense-mediated decay (NMD) pathway. Nonsense-mediated mRNA decay (NMD) is a mechanism for quickly removing mRNAs containing a premature termination codon, as well as a regulatory pathway for numerous genes such as c-Myc (Li et al. 2015). NMD is an essential mechanism for RNA quality control and gene regulation in eukaryotes as shown in Figure 1.4. Activation of NMD mechanism results in mRNA degradation reduction in mRNA levels (Nickless et al. 2017). NMD can therefore protect cells by eliminating mutant transcripts that generate dominant-negative proteins. On the other hand, if the truncated protein is partially functional, the degradation of the transcripts can result in more severe conditions.

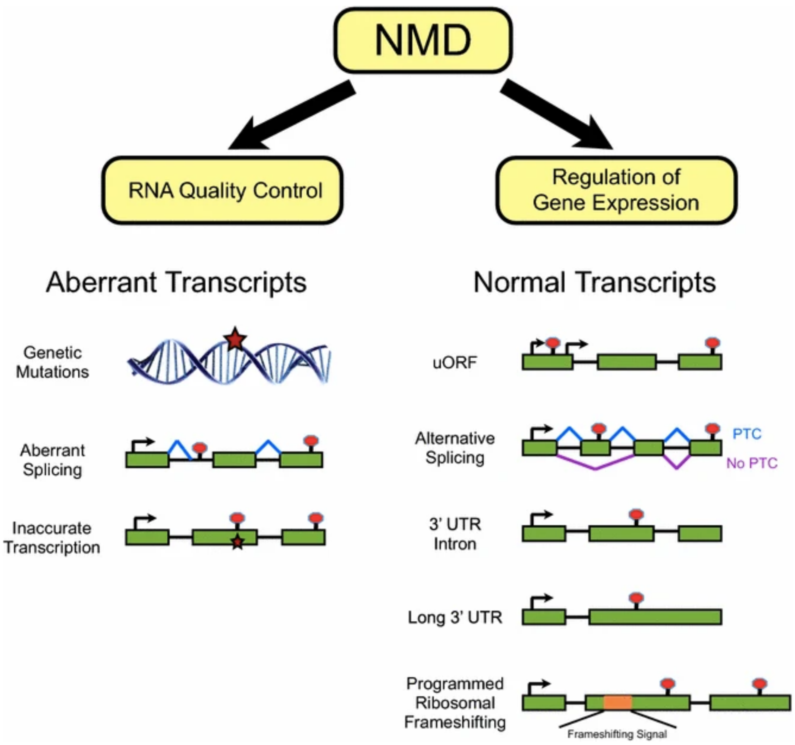

Figure 1.4: NMD is involed in both RNA maintenance and gene regulation (Nickless, 2017).

1.4 Regulation of *ATP13A2* Gene

The information regarding the regulation of *ATP13A2* gene expression in the literature is very limited however there is an important link between the regulation of *ATP13A2* through the PHD2-HIF1α signaling pathway and the crucial role it plays in cellular iron homeostasis (Rajagopalan et al., 2016). In a conserved complex, HIF1α transcription factor regulates the expression of neuroprotective genes involved in cellular stress responses, including those that regulate iron homeostasis (Siddiq et al., 2005). Knowing the critical role of ATP13A2 on iron transportation within the cells, *ATP13A2* promoter was targeted for the investigation of hypoxia response elements where the transcription factor HIF1α binds to. Several hypoxia response elements were found on the -2000 bp upstream of *ATP13A2* promoter region and binding of HIF1α to *ATP13A2* promoter region was detected. It was also reported that upon stable HIF1α expression, ATP13A2 expression was increased, which supports the information on ATP13A2's essential role on the cellular iron homeostasis (Xu et al., 2012).

1.5 Aim of the Study

During this study, effects of the c-Myc transcription factor on the *ATP13A2* gene expression was investigated. *ATP13A2* gene is associated with rare neurodegenerative diseases such as PD and KRS. There are limited studies on the transcriptional regulation of *ATP13A2*, and how it is regulated by which transcription factors remains mostly unknown. In the study that was previously done in our laboratory with the novel homozygous mutation c.1422_1423del:p.P474fs ATP13A2 mutation, it was found that the mutated ATP13A2 mRNA was degraded by NMD, a post-transcriptional regulation mechanism as a result of the mutation, and the expression level of mutant ATP13A2 increased when a known NMD suppressive agent 5-azacytidine was applied (Kırımtay et al., 2020). In addition, it was observed that the expression level of wild-type ATP13A2, which is not targeted by the NMD mechanism, was also increased upon 5-azacytidine administration. Also, it is known that 5-azacytidine both decreases global methylation and increases c-Myc expression, and allows c-Myc to bind demethylated CACGTG (E-Box) sequences. Based on these results, it was suggested that the *ATP13A2* gene might be regulated by c-Myc. It was also determined that there are many E-Box-similar sequences present in the *ATP13A2* promoter with the bioinformatics analyzes performed.

By conducting this research, it was aimed to confirm the c-Myc transcription factor binding and uncover its possible effects on ATP13A2 expression. C-Myc binding was determined by using chromatin immunoprecipitation assay and the effects of c-Myc overexpression on ATP13A2 expression was measured by luciferase assay. Furthermore, qRT-PCR method was used in order to confirm the luciferase assay results by measuring the mRNA expression levels of ATP13A2 upon overexpression of c-Myc transcription factor. Additionally, changes in the ATP13A2 protein levels due to c-Myc overexpression were aimed to be determined by western blot analysis in both c-Myc overexpressed HEK239T cells and KRS patient fibroblasts.

2. MATERIALS AND METHODS

2.1 Materials

2.1.1 Bioinformatics tools

The names of the websites, reasons for using the said software and website URL of the tools are listed in Appendix B.

2.1.2 Instruments

All of the instruments and electronic devices that are used in this study, are listed in Appendix B.

2.1.3 Equipment:

All of the laboratory equipment used in this research are given in Appendix B.

2.1.4 Buffers, chemicals and solutions

2.1.4.1 Commercially available solutions

All of the commercially purchased solutions and chemicals used in this study are given in Appendix B.

2.1.4.2 Prepared chemicals and solutions

All of the prepared solutions and buffers are given in Appendix C.

2.1.5 Bacterial culture

2.1.5.1 Bacterial culture solutions

LB broth

In order to grow the competent bacteria, LB broth was prepared as written in Table 2.1. After preparing the mixture, the solution was autoclaved at 121 °C for 15 minutes for sterilization. Once the solution cooled down at room temperature, 50 µg/ml ampicillin was added before the transformed bacteria was grown in 37 °C, on a shaking incubator.

Table 2.1: LB-broth preparation recipe.

Contents	Amounts
Tryptone	5 g
Yeast extract	2.5 g
NaCl	5 g
dH_2O	up to 500 ml

LB-agar plate

The ingredients needed to prepare the LB-agar plates are given in Table 2.2. After preparing the mixture, the solution was autoclaved at 121 °C for 15 minutes. Once the solution cooled down around 55-60 °C, 50 µg/ml ampicillin was added and 10 ml LB-agar solution was poured into 100 mm petri plates for bacterial seeding.

Table 2.2: LB-agar preparation recipe.

Contents	Amounts
Tryptone	5 g
Yeast extract	2.5 g
Agar	7.5 g
NaCl	5 g
dH2O	up to 500 ml

2.1.6 Commercial kits

All of the commercially available kits used during this research are given in Table 2.3.

Table 2.3: Commercial kits and the supplier company names.

Commercial Kits	Company
BCA Protein Assay Kit	Thermo Scientific
NucleoSpin® RNA Isolation Kit	Macherey-Nagel
LightCycler® 480 Probes Master	Roche
ProtoScript® II First Strand cDNA Synthesis Kit	New England Biolabs
Dual-Luciferase® Reporter Assay System	Dual-Luciferase® Reporter Assay System

2.1.7 Antibodies

All of the antibodies used during this research are given in Table 2.4. Antibodies used for western blotting experiments are diluted in 5% milk powder blocking solution according to the manufacturer's recommendations.

Table 2.4: Antibody and the supplier company names.

Antibody Name	Company
ß-actin Mouse mAb	CST
Anti-DYKDDDDK (FLAG) Tag Mouse mAb	CST
IRDye® 800CW Rabbit IgG (H + L)	LI-COR
IRDye® 680RD Mouse IgG (H + L)	LI-COR
Anti-ATP13A2 antibody	Santa Cruz
Anti- HIF1α antibody	CST

2.1.8 Cell culture cells and media

2.1.8.1 HEK293 cell line

Human embryonic kidney 293 cells (HEK293) are an immortalized cell line derived in 1973 from human embryonic kidney cells produced in tissue culture from a fetus of a female (Kavsan, 2011). They were mainly chosen for the c-Myc overexpression experiments due to being readily available for transfection, they are relatively low-maintenance and divide extremely rapidly (Thomas et al., 2005). Most importantly, they are also extremely efficient at producing recombinant proteins that are produced from plasmids with CMV promotors due to adenoviral genes being incorporated into HEK genome (Graham et al., 1997).

2.1.8.2 Primary fibroblast cells

Previously in our laboratory, skin samples taken from KRS patients and healthy control individuals using punch biopsy method were used to establish primary fibroblast cell cultures (Kırımtay et al., 2020).

2.1.8.3 Cell culture media

Primary fibroblast cells and HEK293Tcells were both cultured in Dulbecco's Modified Eagle Medium (DMEM), supplied with 10% Fetal bovine serum (FBS), 1X Penicillin/Streptomycin and followed by filtration (0.22 µm) for sterilization.

For fibroblasts, during the initial thawing and seeding of the cells, DMEM with 20% FBS was used until the cells attached to the preferred cell culture dish since it was observed that using 20% FBS increased the cell viability of primary fibroblast cells, compared to other primary fibroblasts stocks that were thawed and seeded using DMEM that was supplied with 10% FBS.

2.1.9 Vectors

2.1.9.1 3X-FLAG-CMV-10 plasmid

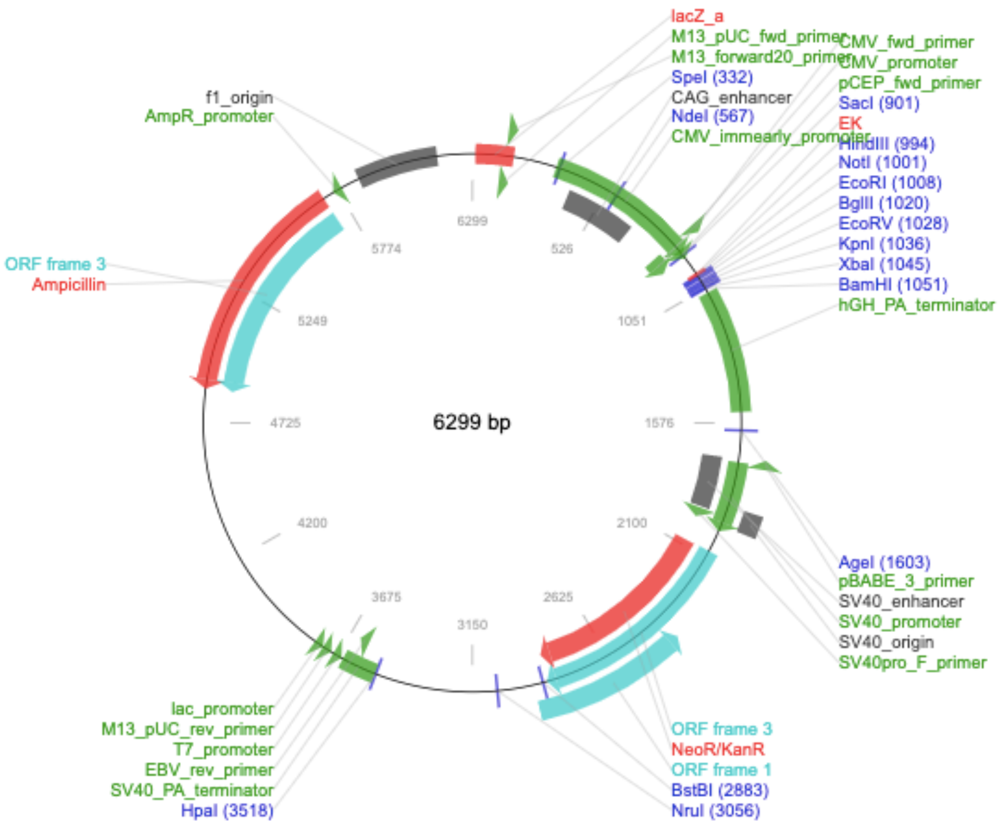

Figure 2.1: p3xFLAG-CMV-10 vector map.

The p3xFLAG-CMV-10 vector (Figure 2.1) was used in order to function as an expression vector for mammalian cells. *C-Myc* gene was cloned inside the p3xFLAG-CMV-10 vector by using EcoRI and BamHI restriction enzymes.

2.1.9.2 pGL3-Basic vector plasmid

The pGL3-Basic vector (Figure 2.2) was used for the process of cloning *ATP13A2* promoter region in order to be used in the Luciferase assay.

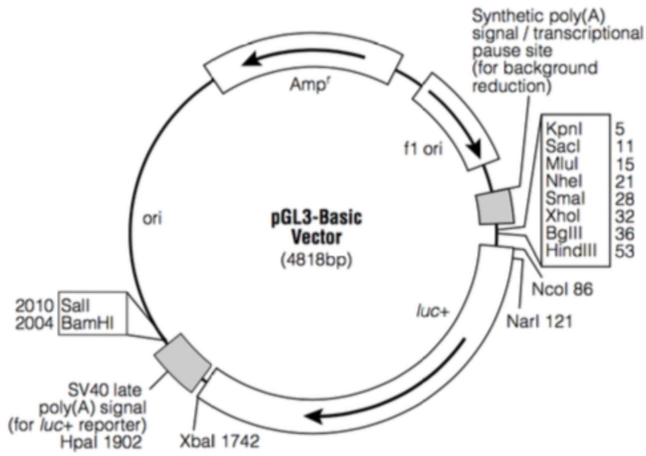

Figure 2.2: pGL3-Basic vector map.

2.1.9.3 pRL-TK vector

The pRL-TK vector (Figure 2.3) was used as an internal control during the Luciferase assay.

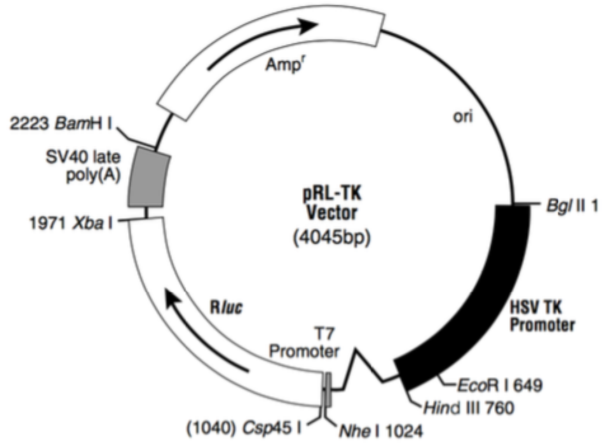

Figure 2.3: pRL-TK vector map.

2.2 Methods

2.2.1 Bioinformatic analysis

TFBIND Web Software and MATCH were used in order to determine potential c-Myc binding sites located on the *ATP13A2* promoter region.

The determined binding sites were targeted for ChIP primer designing. *ATP13A2* promoter sequences were obtained from UCSC Genome Browser. c-Myc coding sequence was obtained from NCBI CCDS database. In order to clone the promoter sequence and c-Myc gene into expression vectors, primers were designed using OligoAnalyzer 3.1.

2.2.2 Cloning of *c-Myc* gene

For the cloning process, total RNA was isolated from HEK293 cells, which express c-Myc according to the Human Protein Atlas data, and the obtained RNA was converted into cDNA with the ProtoScript® II First Strand cDNA Synthesis Kit.

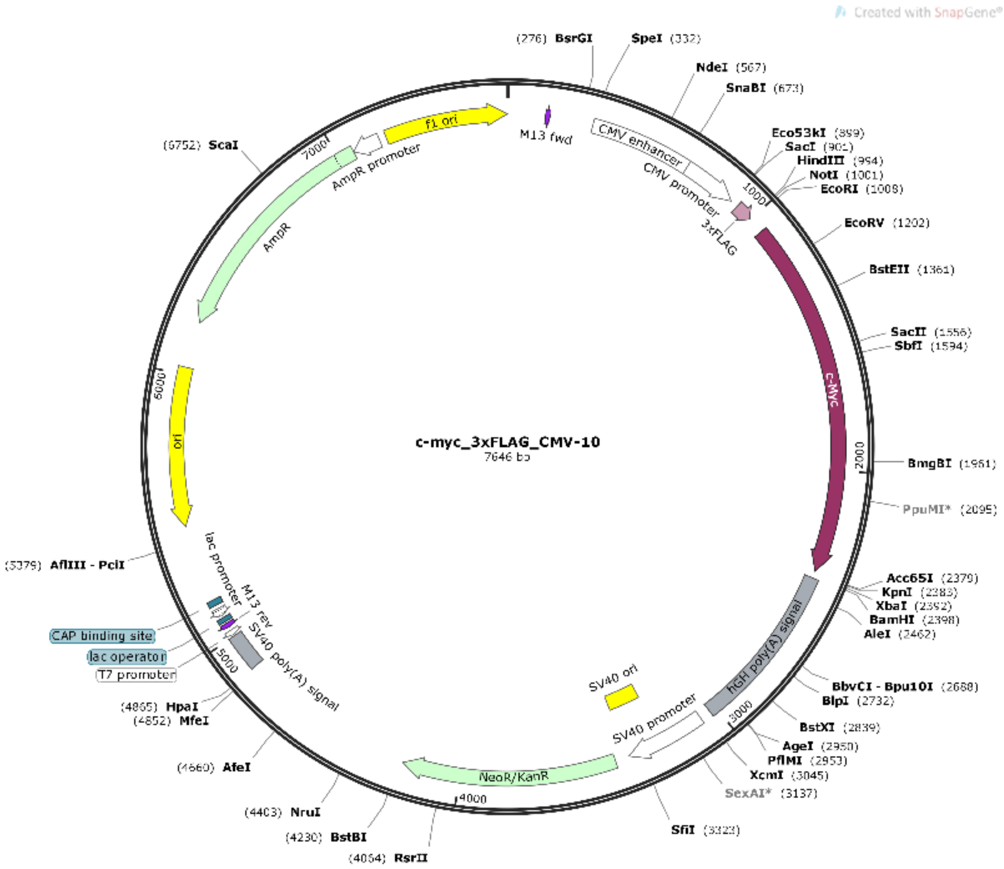

Figure 2.4: p3xFLAG-CMV10 vector map with *c-Myc* gene cloned inside.

Then, using the cDNA as a template, the *c-Myc* coding sequence was amplified with the Q5 High Fidelity DNA polymerase enzyme through the primers given in Table 2.5.

The resulting amplicons and the 3xFLAG_CMV-10 vector were cut with the EcoRI and BamHI enzymes, and then the c-Myc amplicon cut with DNA ligase was transferred to the 3xFLAG_CMV-10 vector to create the c-Myc expression vector shown in Figure 2.4. The *c-Myc* sequence that was cloned in the vector was confirmed by Sanger sequencing.

The sequenced data was aligned using the ENSEMBL reference sequence to determine any possible point mutations that could have occurred during the PCR step. Sequence alignment is shown in Appendix A.

Table 2.5: c-Myc cloning primers for p3xFLAG-CMV-10.

	Sequence (5' -> 3')	Length	Tm
C-myc_F_ primer	AAAAAGAATTCCTGGATTTTTTTCGGGTAGTGG	33	57.57
C-myc_R_primer	TTGGTACCTTACGCACAAGAGTTCCGTAG	29	58.06

2.2.3 Cloning of *ATP13A2* promoter region

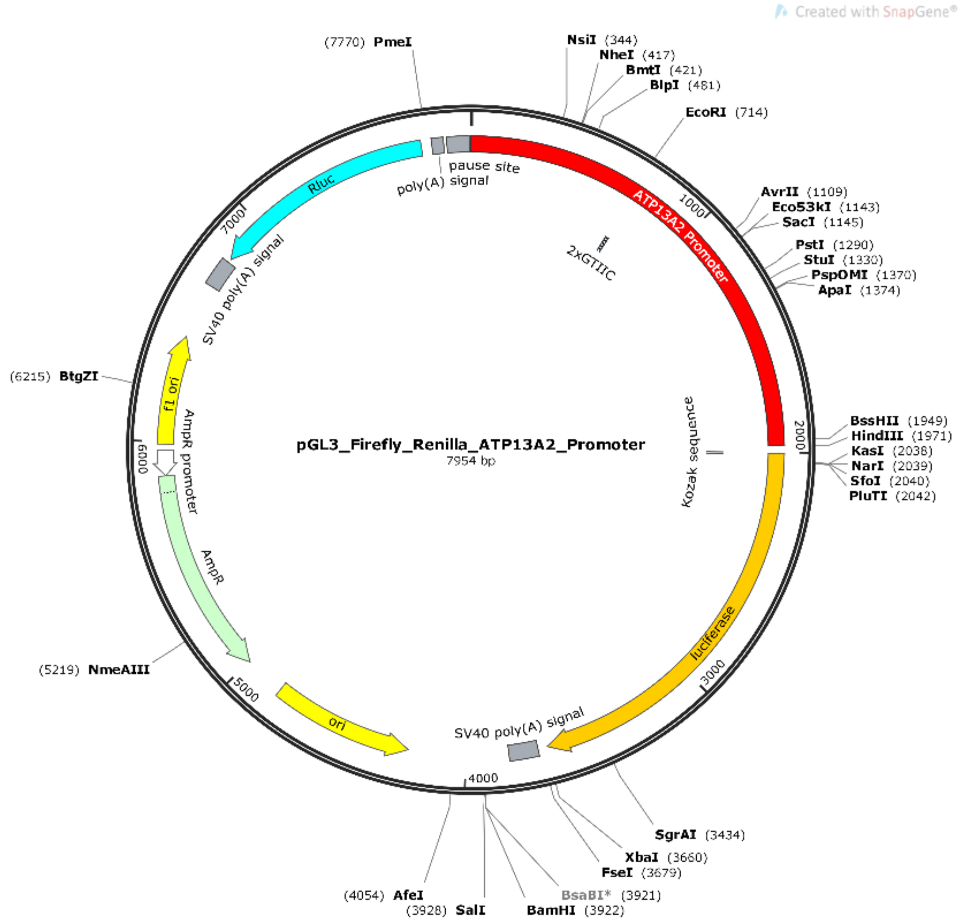

Figure 2.5: pGL3-Firefly-Renilla Vector with *ATP13A2* promoter region cloned inside.

pGL3_Firefly_Renilla vector, which would enable expression of both firefly luciferase and renilla luciferase enzymes from a single plasmid to minimize experimental bias. For cloning, the *ATP13A2* promoter region was amplified from genomic DNA isolated from HEK293T cells, with the Q5 High Fidelity DNA polymerase enzyme with the primers specified in Table 2.6. Then, both the promoter amplicon and the pGL3_Firefly_Renilla vector were cut with the restriction enzymes XhoI and HindIII, and the *ATP13A2* promoter sequence was inserted just before the Firefly luciferase gene with DNA ligase to obtain the vector shown in Figure 2.5.

ATP13A2 promoter sequence was confirmed by Sanger sequencing after the cloning process was successfully completed.

Table 2.6: *ATP13A2* cloning primers for pGL3 vector.

	Sequence (5'->3')	Length	Tm
*ATP13A2*_Promoter_F	AAGGTACCATGCAGTCCCCAAGCCCTC	27	61.99
*ATP13A2*_Promoter_R	AAAAAGCTTACTGCCGCAGTCCCTCCG	27	64.42

2.2.4 Chromatin immunoprecipitation assay

Chromatin Immunoprecipitation assay (ChIP) was done by using SimpleChIP® Enzymatic Chromatin IP Kit. Experimental steps were all conducted based on the manufacturer's manual.

2.2.4.1 Crosslink and chromatin digestion

$4x10^7$ HEK293T cells were crosslinked and fragmented per the SimpleChIP® Enzymatic Chromatin IP Kit instructions. The MS-72 probe was used to disrupt the nuclear membrane; the fragmented chromatin sample was stored at -80 °C.

2.2.4.2 Chromatin digestion analysis

50 µl of chromatin that had been digested and that was stored at -80 °C, was analyzed before the immunoprecipitation step per the manufacturer's instructions. The purpose of this analysis was to ensure the success of DNA fragmentation prior to the IP steps.

2.2.4.3 Immunoprecipitation

Following the instructions of SimpleChIP® Enzymatic Chromatin Immunoprecipitation (IP) Kit, for each IP reaction, 1X ChIP buffer was prepared. Approximately 5 µg DNA was used per IP reaction.

During the IP reactions, FLAG antibody was used for targeting overexpressed c-Myc transcription factor, Histone 3 (H3) antibody is used as a positive control where normal Rabbit IgG antibody is used as a negative control. Also, to determine non-specific binding of the DNA to the magnetic beads, another recommended control condition was for incubating the fragmented DNA samples without the antibody addition and performing the IP with just the magnetic beads that were supplied in the ChIP kit as another negative control.

IP reactions were incubated for 3 hours in order to minimize the nonspecific binding of Flag tagged c-Myc protein. After the incubation period 30 µl ChIP-Grade Protein G Magnetic Beads are added to the samples. Magnetic Beads and the IP reaction mixture was incubated for 2 hours. Once the magnetic bead incubation period was over, the samples were washed three times with the 1ml low salt wash buffer and once with 1ml high salt wash buffer, using the magnetics separation rack in between the washes. Samples were each incubated on the rotator for 5 minutes with 5 rpm during each wash. After the washes were completed, the magnetic beads were treated with 150 µl 1X ChIP elution buffer.

Samples including the elution buffer were incubated on the shaking heat block for 30 minutes at 65 °C. The input sample was also mixed with 150 µl elution buffer and incubated at room temperature. At the end of the incubation time, the magnetic separation rack was used to separate the eluted chromatin into new tubes. Each sample was treated with 6 µl 5M NaCl and 2 µl Proteinase K then incubated at 65 °C for 2 hours.

Once the chromatin samples were done with incubation, they were purified as the SimpleChIP® Enzymatic Chromatin IP Kit recommendations. Purified samples were then used for the PCR step, in order to detect the binding sites of c-Myc transcription factor on *ATP13A2* promoter region.

2.2.4.4 PCR

PCR was done in order to amplify the *ATP13A2* promoter fragments that included c-Myc binding sites. The primers were designed using OligoAnalyzer 3.1 tool by calculating the GC content, annealing temperatures and self-dimer formation. Sequences, lengths of the targeted amplicons, primer lengths and calculated melting temperatures are shown in Table 2.7.

These primers were also confirmed by using NCBI's Primer-BLAST tool to check if their binding sites were specific to *ATP13A2* promoter region only. The designed primers were purchased from PRZ Biotech.

PCR experimental conditions are given in Table 2.8 and Table 2.9 respectively. Also, positive control histone H3 rabbit monoclonal antibody, negative control normal rabbit IgG antibody, and primer sets for ribosomal protein L30 (RPL30) gene locus PCR detection (human and mouse primer sets) were included in the ChIP kit.

Table 2.7: *ATP13A2* promoter primer pairs that target c-Myc binding sequences for ChIP assay.

Primers	**Length of amplicon**	**Sequence 5'->3'**	**Primer length**	**Tm**
*ATP13A2*_ChIP_F1	195	TCCAGCCCCTTCCACAATAG	20	59.08
*ATP13A2*_ChIP_R1		GATAGACGTGGGCAGGATCA	20	58.96
*ATP13A2*_ChIP_F2	186	GCACGCAGGTAAGACATCTC	20	58.72
*ATP13A2*_ChIP_R2		ACCTGCCCAGAGATTCACAG	20	59.38
*ATP13A2*_ChIP_F3	200	GAGTAAATGGCTCCACTGGC	20	58.62
*ATP13A2*_ChIP_R3		AGGGTGTGGGTAGGGGATAG	20	59.73
*ATP13A2*_ChIP_F4	199	TTGGGAAAAGAGGGCCAGAG	20	59.59
*ATP13A2*_ChIP_R4		GCTGCCGGGACTTGTAGT	18	59.34
*ATP13A2*_ChIP_F5	150	CCTCCCCTGGAAGTGTCAC	19	59.32
*ATP13A2*_ChIP_R5		GTGCCAGTGGAGCCATTTAC	20	59.19
*ATP13A2*_ChIP_F6	198	TGATGCCAGAACCCAGCC	18	59.64
*ATP13A2*_ChIP_R6		TCTTCCGGTGACACTTCCAG	20	59.32

Cellular chromatin contains histone H3, which binds to most DNA sequences, including the RPL30 region. Thus, histone H3 rabbit monoclonal antibody immunoprecipitation of chromatin will form a positive band for the RPL30 gene primers, but conventional rabbit IgG antibody will not.

In order to show that the IP reaction works, H3 antibody can be used with the RPL30 primer sets included in the kit for a conventional PCR. Running the H3 RPL30 PCR reaction in the agarose gel and detecting of the specific band that the kit recommended can be interpreted as the positive control of the IP reaction. Rabbit IgG antibody PCR reaction will serve as the negative control since theoretically, IgG antibody will not bind to any fixated DNA fragment during IP reactions thus it should not produce a positive IgG band when the PCR reaction, that is set up using the DNA obtained from the IP reaction, is run in the agarose gel.

After completing the PCR reactions for each IP sample, amplicons were visualized using 1X Sodium Borate Buffer for the agarose gel. MassRuler Low Range DNA Ladder was loaded alongside with the PCR products since the expected amplicon sizes are approximately between 150-200 base pair. The gel was run at 250 V for 15 minutes and the gel was visualized using the Bio-Rad ChemiDoc Imaging System.

Table 2.8: PCR components for ChIP amplicons.

Component	Volume	Final Concentration
dNTP mix (10 mM)	0.4 µl	0.2 mM
Forward primer (10 µM)	1 µl	0.5 mM
Reverse primer (10 µM)	1 µl	0.5 mM
Template DNA	1 µl	5 ng
Taq Polymerase	0.2 µl	1 U
10X Taq Pol. Buffer	2.5 µl	1X
Nuclease-free H2O	Add up to 25µl	-

Table 2.9: PCR conditions for ChIP amplicons.

Step	Temperature	Time
Initial Denaturation	95°C	30 sec
Denaturation	95°C	10 sec
Annealing	58-60°C	20 sec (25 cycles)
Extension	72°C	15 sec
Final Extension	72°C	5 min

2.2.5 Cell culture methodology

2.2.5.1 Seeding stock cells

HEK293T cells

HEK293T stock cells were thawed and immediately supplemented with 4 ml of HEK293T culture medium DMEM, then centrifuged at 1500 rpm for 5 minutes. The cell pellet was dissolved in 1 ml of fresh growth medium and then seeded in cell culture flasks in approximately 6 ml culture media.

Primary fibroblast cells

In our laboratory, primary fibroblast culture was previously established from samples taken from KRS patients and healthy individuals as control (Kırımtay et al., 2020). Frozen stock cells from previous studies were removed from -80 °C and thawed in a 37 °C water bath. In order to ensure their survival, upon the initial seeding, the fibroblasts were supplemented with DMEM prepared with 20% FBS and 1%

penicillin-streptomycin. Cells were centrifuged at 1500 rpm for 5 minutes. The pellet was dissolved in 2 ml of fresh growth medium and then seeded in cell culture flasks.

2.2.5.2 Cell counting and passaging

HEK293T cells

When HEK293T cells reached the 70-80% confluency, the previous cell culture media was discarded. Remnants of the cell culture media were washed away with filtered 1X PBS. The cells were detached with 2 ml Trypsin for T-75 cell culture flasks. The cells were then incubated in 37 °C, 5% CO_2 culture incubator for 5 minutes. Once the cells were detached, the Trypsin enzyme was inactivated by adding 4 ml cell culture media inside the flasks.

The cell suspension was collected into a 15 ml falcon and centrifuged at 1500 rpm for 5 minutes. The supernatant was discarded and the cell pellet was dissolved in 2 ml growth medium.

For determining the number of the cells, cell suspension and trypan blue dye was mixed with a 1:1 ratio and was put onto a hemocytometer and the cells on 25 square (1 mm^2) were counted. After determining the cell number, $1x10^6$ cells were seeded into a clean T-75 cell culture flask with the 8 ml final cell culture medium volume.

Primary fibroblast cells

When fibroblast cells reached the 70-80% confluency, the previous cell culture medium was discarded. Remnants of the cell culture media were washed away with filtered 1X PBS. The cells were detached with 3 ml Trypsin for T-75 cell culture flasks. The cells were incubated in 37°C, 5% CO^2 culture incubator for 15 minutes. Fibroblasts cells require more incubation time to detach compared to HEK293T cells.

Once the fibroblasts were detached, the Trypsin enzyme was inactivated by adding 6 ml cell culture media inside the flasks. The cell suspension was collected into a 15 ml falcon and centrifuged at 1500 rpm for 5 minutes. The supernatant was discarded and the cell pellet was dissolved in 1 ml growth medium.

For determining the number of the cells, 10 µl of cell suspension was mixed with 10 µl trypan blue and was put onto a hemocytometer and the cells on 25 square (1 mm^2) were counted. The number of cells were calculated. After determining the cell number,

$1x10^6$ cells were seeded into a clean T-75 cell culture flask with the 8 ml final cell culture medium volume.

2.2.6 qRT-PCR

2.2.6.1 Transfection of HEK293T cells

For protein expression analysis, linear PEI, a cationic polymer, was used for the HEK293T cells. In our experience, HEK293T cells are easily transfected using PEI. The optimal quantity of PEI was determined on the cell line. In our laboratory, the optimal ratio of DNA to PEI for HEK293T cells was determined to be 1:3.

2.2.6.2 RNA isolation and cDNA synthesis

For qRT-PCR analysis, total RNA was isolated from cells using the MN NucleoSpin RNA kit. The concentration of isolated RNA was measured suing NanoDrop. The cDNA library was generated using the ProtoScript® II cDNA Synthesis kit. The resulting cDNAs were used according to the manufacturer's instructions in the Light Cycler 480 Probe Master qRT-PCR kit. For qRT-PCR reactions, human-specific *ATP13A2* probe (UPL#5) and primers (Forward: 5'-CATACCGGTCAAGTCCTACCC and Reverse: GCACAGGGCGTACCAGTAGT) were used for the ATP13A2 mRNA expression detection. The human-specific *HIF1α* probe (UPL#130) and primers (Forward:5'- TATGGTTCTCACAGATGATGGTGAC -3' and Reverse 5'- CCTCATGGTCACATGGATGAGTA -3') were used for the *HIF1α* mRNA expression detection. Expression of human *beta-actin* (Roche) was used as a control for relative expression analysis. Normalization of qRT-PCR data will be performed using the ΔΔCT method, and its statistical significance was evaluated using the student's t-test. If the p value was less than 0.05, the difference between the two categories was considered to be statistically significant. The qRT-PCR reactions for each condition were performed in triplicates, and the experiment was repeated at least three times.

2.2.6.3 qRT-PCR reaction mix

The qRT-PCR reaction master mix was prepared according to the manufacturer's instructions in the Light Cycler 480 Probe Master qRT-PCR kit. 5 µl of cDNA was put in each qRT-PCR strip and 15 µl of reaction master mix was distributed on each well.

The strips were covered with the seal cap and the tubes were put in the spinner to ensure all of the reaction is located at the bottom of the strip tubes with no bubbles. After the spinning process, the strips were loaded into Light Cycler 480 Instrument. PCR program was selected and the program was started as stated in Table 2.10.

Table 2.10: qRT-PCR program for *ATP13A2* and *actin* probes.

Programs	Target	Hold	Cycle
Pre-incubation	95°C	10 min	1
Amplification	95°C 60°C 72°C	10 sec 30 sec 1 sec	45
Cooling	40°C	30 sec	1

2.2.7 Luciferase reporter assay

Luciferase assay was performed to examine the regulation of the *ATP13A2* promoter by the c-Myc transcription factor, using the Dual-Luciferase® Reporter (DLR) Assay System (Promega). The conditions created within the scope of the experiment are as follows:

• As negative control, empty pGL3_Firefly_Renilla vector and empty 3xFLAG_CMV_10 vector or the 3xFLAG_CMV_10 vector containing c-Myc were transfected into cells.

• As the experimental group, together with the pGL3_Firefly_Renilla vector containing the ATP13A2 promoter, an empty 3xFLAG_CMV_10 vector or 3xFLAG_CMV_10 vector containing c-Myc were transfected into the cells.

Each condition was also transfected with the internal control vector, pRL-TK.

2.2.7.1 Transfection of HEK293T cells

A cationic polymer-based method was used for the transfection process and polyethyleneimine (PEI) was preferred as the cationic agent. Using 3 µl of PEI for 1 µg of DNA was the condition optimized for this experiment and cell line in our laboratory.

Cells were seeded into 24-well plates as $3x10^4$ cells and transfection was performed 24 hours after the seeding of the cells. 600 ng of pGL3-Basic/pGL3-*ATP13A2* promoter vector, 300 ng of p3xFLAG-CMV-10/p3xFLAG-*cMyc* transcription factor vector, 30 ng of pRL-TK internal control vector is transfected. Transfection ratios for each experimental condition are given in Table 2.11.

Table 2.11: Transfection conditions for dual luciferase assay.

	pGL3 Basic	**pGL3-*ATP13A2***	**3xFLAG-CMV-10**	**3xFLAG-cMyc**	**pRL-TK**	**PEI**
1: PGL3 basic -mock	600ng	x	300ng	x	30ng	8.37µl
2: *ATP13A2* promoter - mock	x	600ng	300ng	x	30ng	8.37µl
3: PGL3 basic -*c-Myc*	600ng	x	x	300ng	30ng	8.37µl
4: *ATP13A2* promoter - *c-Myc*	x	600ng	x	300ng	30ng	8.37µl

2.2.7.2 Luminometrical measurement

For the luciferase assay, 48 hours after transfection, cells were lysed with 60 µl of 1X Passive Lysis Buffer to collect proteins and first measure the Firefly luciferase reporter by adding 50 µl of Luciferase Assay Reagent II (LAR II) to generate a stabilized luminescent signal. After measuring the Firefly irradiation, the Renilla luciferase irradiation was measured by adding 50 µl of Stop & Glo® Reagent to the same sample. After obtaining the numerical data, the value for Firefly was proportioned to the value for Renilla, then the experimental groups were normalized with the negative control group and the possible difference was calculated in terms of fold change using Equation 2.1.

Measurements were performed with a Fluoroskan Ascent FL luminometer (Thermo). Each condition was performed in triplicates and the experiments were repeated at least three times on different days. The data obtained from the experiments were tested with ANOVA multiple comparison analysis for statistical significance and the difference between conditions were considered significant for the case where the p value was less than 0.05.

$$\Delta^{\text{Fold activation}} = \frac{Average\left(\frac{Firefly}{Renilla}\right) Sample\ X}{Average\left(\frac{Firefly}{Renilla}\right) pGL3-basic} \tag{2.1}$$

2.2.8 Western blotting

2.2.8.1 Transfection of HEK293T cells

For protein expression analysis, linear PEI, a cationic polymer, was used for the HEK293T cells. The optimal quantity of PEI was determined based on the cell line. In our laboratory, the optimal ratio of DNA to PEI for HEK293T cells was determined to be 1:3. For western blotting, 10 µg of plasmid DNA(3XFLAG-CMV-10_cmyc) was mixed with 30 µg of PEI for the transfection of HEK293T cells on a 100 mm cell culture dish.

2.2.8.2 Nucleofection of patient fibroblasts

Nucleofection of primary fibroblast cells was done by using Amaxa® Cell Line Nucleofector®. In order to perform the nucleofection, first, the fibroblast cells were detached and cell density was determined. $1x10^6$ cells were put in a separate tube and centrifuged at 1200 rpm for 5 minutes. After the supernatant was discarded, 10 µg of plasmid DNA containing *c-Myc* gene is placed on top of the cell pellet. Afterwards, the cell pellet and the plasmid DNA were dissolved in the nucleofection buffer, Cell/buffer suspension was placed into the cuvette and cuvette was placed on the device. Program O-007 was chosen and the nucleofection was started. As soon as the nucleofection process was ended, 1 ml medium was added to each sample cuvette and the cells were seeded onto 100 mm cell culture dish.

2.2.8.3 Total protein isolation

After 48 hours of the transfection, the medium on the transfected HEK293T cells were discarded and washed with 3ml 1X PBS. The cells were then collected into 15 ml falcon tubes using cell scrapers. Samples were centrifuged at 4000 rpm for 6 minutes. The supernatant was discarded and the pellet was dissolved in RIPA lysis buffer that was supplemented with protease inhibitor. The samples were incubated on ice for 30 minutes, then they were centrifuged at 11000 rpm for 30 minutes at 4°C. Once the centrifugation was done, supernatant, which contained the total cellular proteins, was collected into new tubes and the pellets were discarded. The protein concentration was measured using BCA assay.

2.2.8.4 SDS-PAGE

SDS-PAGE was made with 10% acrylamide in the separating gel and 5% acrylamide in the stacking gel. The gels' ingredients are listed in Appendix B.

Separating gel was first poured into the gel cassette and the remaining gap was filled with isopropanol to ensure the top of the gel was smooth. Once the gel was set, the isopropanol was carefully washed away with distilled water. After making sure the gap between the gel cassette was dry, the stacking gel is poured above the separating gel and the gel comb was carefully placed. Gel cassette system was left to polymerize completely before proceeding with the sample loading.

After the gel was set, the gel was placed into the frame, inside the electrophoresis tank. The electrophoresis tank and the inside of the gel frame were filled with 1X SDS running buffer. Protein samples were thawed on ice and the gel loading samples were prepared by mixing the desired amount of protein with the 6X protein loading dye. The samples were denatured at 60°C for 20 minutes instead of 95 °C for 5 minutes. This optimization was done to prevent the ATP13A2 membrane protein to form aggregates instead of denaturing completely. The samples and the molecular weight protein marker were loaded onto the SDS gel and the electrophoresis process was started at constant 30 mA until the sample passed through the stacking gel. Once the sample was on the separating gel, the system was set to constant 100V until the electrophoresis process finished.

2.2.8.5 Western blotting

When the running of the SDS-PAGE was complete, the glass frames holding the gel in place were carefully removed and the gel was washed with dH_2O. Afterwards, both the gel and the nitrocellulose membrane were placed into freshly prepared 1X transfer buffer for approximately 5 minutes. The sandwich system was constructed between the transfer packs and sponges. The transfer cassette was then placed into the tank along with fresh 1X transfer buffer and an ice pack to keep the tank cool throughout the transfer process. Wet transfer was started with 16V, as an overnight incubation in a cold room.

Once the transfer was finished, the gel was discarded and the membrane was stained with Ponceau dye to visualize all the protein bands that were transferred to detect any air bubbles that might have occurred during transfer. The membrane was blocked with 5% milk powder blocking solution prior to primary antibody incubation. The nitrocellulose membrane was incubated with primary ATP13A2 antibody for 48 hours. After the incubation, the membrane was washed 3 times with approximately 5 ml of 1X TBS-T in order to wash the excess non-specific antibody binding away from the membrane. Li-Cor secondary antibodies were used for protein detection. Appropriate secondary antibody was selected and the membrane was incubated in the secondary antibody for an hour in room temperature. Once the secondary antibody incubation was finished, the membrane was washed 3 times with 1X TBS-T once again in order to minimize the non-specific binding of secondary antibodies on the membrane. The membrane was then left to dry for approximately and hour prior to visualization. Imaging system, Li-Cor Odyssey Clx was used for visualization and the analysis of the western blot assay.

3. RESULTS

3.1 Bioinformatics Analysis of c-Myc Binding Sites on *ATP13A2* Promoter Region

3.1.1 Determination of c-Myc binding sites on *ATP13A2* promoter region

Several potential binding sites (E-boxes) of the Myc-Max complex were identified within 2000 bp of the transcription start site on the *ATP13A2* promoter as shown in Figure 3.1. Potential binding sites were analyzed using TFBIND Web Software and highest scored 8 binding sites were targeted for chromatin immunoprecipitation (ChIP) assay primer design as shown in Table 3.1. Primers were designed for the highest scored 8 binding sites. Primer pairs F3/R3 and F6/R6 were designed to include 2 different potential binding sites that are relatively close to each other on the *ATP13A2* promoter region.

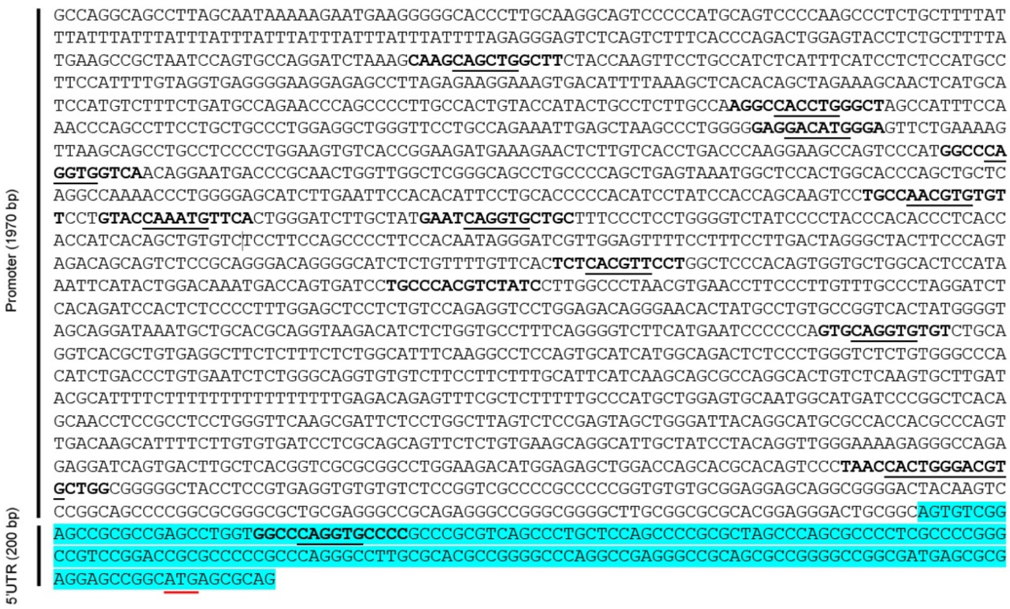

Figure 3.1: *ATP13A2* promoter region sequence. The nucleotide sequence of the 1970 bp promoter region and the 200 bp 5' UTR region of the *ATP13A2* gene is shown. c-Myc binding sequences are shown in bold and underlined. The 5'-UTR region is marked in blue.

Table 3.1: c-Myc binding sites Detected in *ATP13A2* Promotor by TFBIND Web Software.

Name	Score	Location	Motif	Sequence	Target Primer Pair
MYC	0.824796	-978	NANCACGTGNNW	TCTCACGTTCCT	F1/R1
MYC	0.815053	-1373	NNACCACGTGGTNN	GGCCCAGGTGGTCA	F5/R5
MYC	0.810612	-1190	NANCACGTGNNW	TACCAAATGTTC	F3/R3
MYC	0.802206	-1476	NANCACGTGNNW	GAGGACATGGGA	F6/R6
MYC	0.798179	-1564	NNACCACGTGGTNN	AGGCCACCTGGGCT	F6/R6
MYC	0.793538	-696	NANCACGTGNNW	GTGCAGGTGTGT	F2/R2
MYC	0.789861	-1207	NANCACGTGNNW	GCCAACGTGTGT	F3/R3
MYC	0.755329	-172	NNACCACGTGGTNN	CTGGGACGTGCTGG	F4/R4

3.1.2 Determination of the binding Sites on *ATP13A2* promoter by ChIP

In order to detect the binding sites of c-Myc on the 2000 bp *ATP13A2* promoter site, ChIP assay was performed. Before starting with the fragmentation process, the expression of c-Myc gene in HEK293T cells was controlled with western blot. The overexpressed c-Myc protein was detected by using FLAG antibody. β-Actin antibody was used as the western blot loading control. The FLAG-tagged c-Myc protein can be observed around approximately 65 kDa (Figure 3.2).

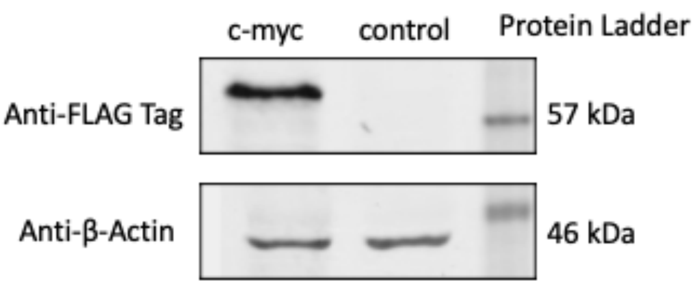

Figure 3.2: The c-Myc overexpression on can be observed in lane 1. Untransfected cell lysate can be observed in lane 2. Prestained Protein ladder can be observed at lane 3.

After observing the c-Myc expression on western blot, the ChIP assay was performed. During ChIP assay, chromatin fragmentation was evaluated by agarose gel electrophoresis continuing with IP reactions. The DNA fragments were mostly in between 150-1000 bp meaning that the DNA was fragmented enough to continue with the IP reactions (Figure 3.3).

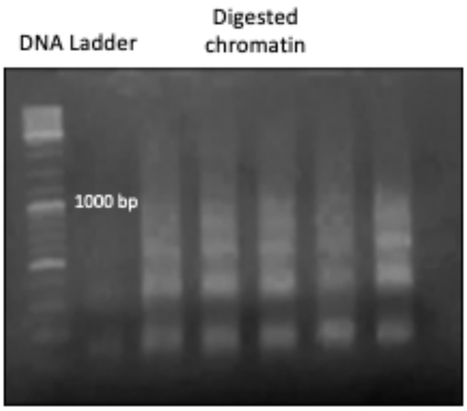

Figure 3.3: HEK293T cells chromatin digestion optimization results shown in 1% agarose gel.

After the fragmentation confirmation, the fragmented DNA was used for the IP reactions. Once the IP reactions were done, the purified DNA sampled obtained from the IP reactions were used for the PCR reactions. IP reactions that were done using the Histone antibody and the Input sample, were used as a positive control while normal rabbit IgG and only bead no antibody IP samples, were used as negative controls.

According to the results of F1/R1 primer pair that targeted the highest scored binding site, which is shown in Figure 3.4, 195 bp long amplicon was detected in the input sample and FLAG antibody IP sample. 161 bp RPL30 amplicon was detected in H3 IP sample, where the H3 positive control PCR reaction was done using *RPL30* gene primers, further confirming the success of the IP reactions.

In the No DNA, IgG and only bead/no antibody (negative control) lanes, no amplicon was detected as expected thus, it can be noted as a significant positive binding site at F1/R1 region.

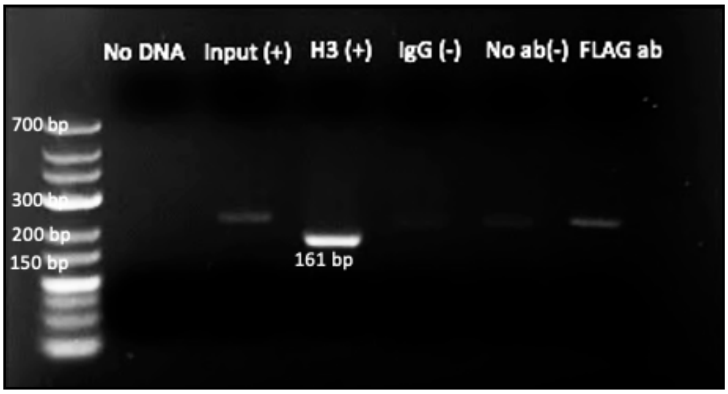

Figure 3.4: PCR results of positive binding at F1/R1 binding site. 5 ng of template DNA was used for each PCR reaction.

For F2/R2 primer pairs, 186 bp long binding site amplicon was detected most prominently in the input sample, along with the H3 positive control amplicon, as expected. However, the bright binding site amplicon band was not as visible in the FLAG antibody IP sample as shown in Figure 3.5.

Based on the comparison between the faint non-specific bands that can also be observed in the IgG and No antibody (No ab) IP reactions, there was no significant binding detected at the F2/R2 binding site.

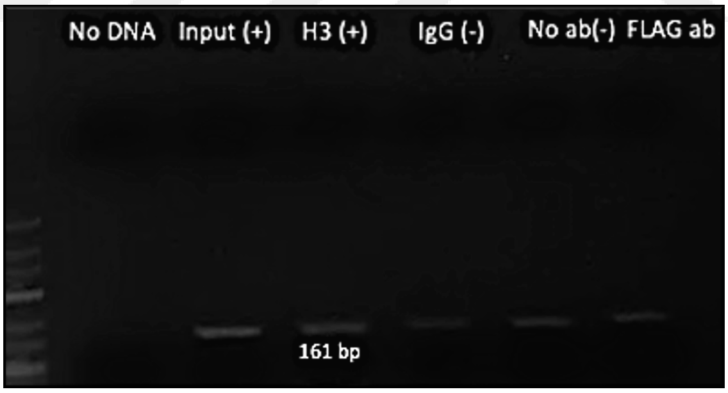

Figure 3.5: PCR results of negative binding at F2/R2 binding site. 5 ng of template DNA was used for each PCR reaction.

Rest of the binding sites were analyzed in a similar fashion and the results are shown in Appendix D. The most significant binding was detected at F1/R1 site while faint binding detections at F3/R3 and F6/R6 were not as prominent compared to the highest scored F1/R1 site. Primer pairs F4/R4 did not work, even under different optimized PCR conditions such as addition of Mg2+ or lowered annealing temperatures. Total detected binding results are given in Table 3.2.

Table 3.2: ChIP assay primer pairs that target *ATP13A2* promoter region and c-Myc binding results based on the conventional PCR/agarose gel results. Green + result shows significant binding where Yellow + results show possible non-specific binding due to F3/R3 and F6/R6 targeting two binding regions within the same primer pair.

F1/R1	F2/R2	F3/R4	F4/R4	F5/R5	F6/R6
+	-	+	Not determined	-	+

3.2 The Effect of c-Myc Transcription Factor on ATP13A2 mRNA Level

Approximately 40-46 hours after overexpressing c-Myc, the mRNA level changes depending on *c-Myc* overexpression levels were measured using qRT-PCR method. Every single experiment was done in triplicates and experiment was repeated 3 different times. During each experiment, the cDNAs were obtained from different RNA samples isolated from mock and c-Myc overexpressed HEK293T cells. The Ct values of each experiment are given in Table 3.3, Table 3.4 and Table 3.5. Control group repetitions labelled as "mock" were the qRT-PCR reactions using the cDNA of HEK293T cells that were transfected with empty 3XFLAG-CMV-10 vector.

Table 3.3: Ct values of experiment N=1.

N=1	ATP13A2	ACTIN
mock	23.94	24.79
	22.82	24.41
	24.22	24.4
c-Myc overexpressed	26.38	24.75
	-	24.8
	26.21	24.15

Table 3.4: Ct values of experiment N=2.

N=2	ATP13A2	ACTIN
mock	22.94	21.87
	21.89	22.44
	22.45	21.57
c-Myc overexpressed	21.99	19.64
	23	18.99
	23.13	-

Table 3.5: Ct values of experiment N=3.

N=3	ATP13A2	ACTIN
mock	20.78	19.44
	19.6	18.91
	20.68	19.03
c-Myc overexpressed	21.54	18.85
	21.52	19
	21.71	18.43

The values of the test results were calculated according to ΔΔCt method. The equations 3.1 and 3.2 are used for the ΔΔCt method fold change calculation (Schmittgen et al., 2008). Control group is normalized as "1" in every experiment.

$$\Delta Ct = 2^{-(Target\ gene - Reference\ gene)} \tag{3.1}$$

$$\Delta\Delta Ct = 2^{-(Test\ \Delta Ct - Control\ \Delta Ct)} \tag{3.2}$$

The fold changes of all of the collective experiments are given in Figure 3.6. All of the results were statistically analyzed with t-test using GraphPad Prism software.

Results of the repeated qRT-PCR experiments indicated that 40-46 hours after the c-Myc overexpression, ATP13A2 mRNA level significantly decreased compared to the control "mock" group.

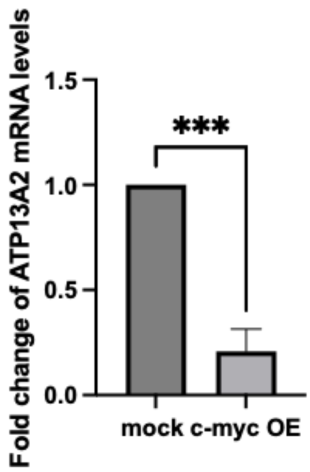

Figure 3.6: Fold change of ATP13A2 mRNA levels, 40-46 hours after c-Myc transcription factor overexpression.

3.3 Determination of the Effects of c-Myc Transcription Factor on *ATP13A2* Expression Level via Luciferase Assay

In order to confirm the qRT-PCR results of c-Myc transcription factor's direct effect on ATP13A2 mRNA levels, dual luciferase assay was performed. HEK293T cells were co-transfected as shown in Table 2.11 and cell pellets were collected approximately 40-46 hours after the transfection.

4 different experimental condition was set up. Transfections including empty pGL3-basic with c-Myc were used for normalization. Δ Fold Activation was calculated using the Equation 2.1 given in methods.

Raw data resulting from 3 different experiments are given in Table 3.6, Table 3.7 and Table 3.8 respectively. Each experiment was conducted at different dates as triplicates. Average value of each replicate within the experiment was taken into the Fold change calculation by taking the average of all of the replicates. The light units that were measured were normalized to internal control values.

Table 3.6: Measured light units resulting from luciferase assay N=1.

N=1	**F1**	**R1**	**F2**	**R2**	**F3**	**R3**
1: PGL3 basic -mock	2.002	2.129	3.018	3.253	2.21	1.972
2: *ATP13A2* promoter - mock	181.9	5.803	139.5	4.748	191.5	6.137
3: PGL3 basic - c-Myc	7.986	8.713	9.954	11.18	10.95	10.87
4: *ATP13A2* promoter - c-Myc	147.2	14.58	158.9	15.79	119.4	13.9

Table 3.7: Measured light units resulting from luciferase assay N=2.

N=2	**F1**	**R1**	**F2**	**R2**	**F3**	**R3**
1: PGL3 basic -mock	5.087	25.53	5	22.75	5.363	26.13
2: *ATP13A2* promoter - mock	545.4	50.23	612.8	54.66	604.2	56.36
3: PGL3 basic - c-Myc	41.06	84.84	52.17	99.84	46.69	95.8
4: *ATP13A2* promoter - c-Myc	659.6	113.2	737.1	112.6	803.4	133.2

Table 3.8: Measured light units resulting from luciferase assay N=3.

N=3	F1	R1	F2	R2	F3	R3
1: PGL3 basic -mock	18.96	78.59	22.02	99.16	20.87	95.83
2: *ATP13A2* promoter - mock	604.6	110.8	745.8	127.7	530.9	91.6
3: PGL3 basic - c-Myc	39.49	108.4	48.18	131.1	45.66	133
4: *ATP13A2* promoter - c-Myc	549.9	169.7	664	194.1	660.7	190.8

The average fold changes are shown in Figure 3.7. The results of luciferase assay indicate that, 40-46 hours after c-Myc transcription factor was overexpressed, it decreased the ATP13A2 expression levels.

These results also aligned with the qRT-PCR data that was previously obtained.

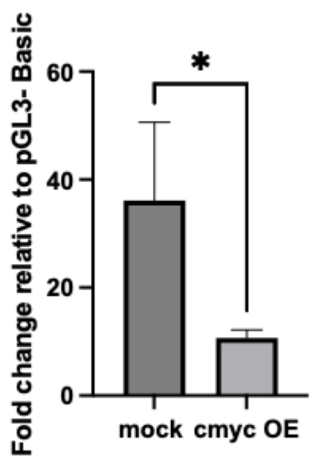

Figure 3.7: Fold changes of normalized light units obtained from the luciferase assay based on c-Myc transcription factor's effect on *ATP13A2* promoter region.

3.4 Determination of the Effect of c-Myc Transcription Factor on ATP3A2 Protein Levels by Western Blotting.

For the western blot experiments, the total proteins from control and c-Myc transfected HEK293T cells were isolated approximately 40-46 hours after transfection. 3 separate cell lysates were used on different days and the statistical analysis was done on the average expression level differences.

Prior to evaluating ATP13A2 protein expression levels, first the overexpression of c-Myc was confirmed by incubating the membrane in FLAG antibody overnight. Once the FLAG-expression was detected in c-Myc transfected cells, the membranes were incubated in primer ATP13A2 antibody for 48 hours. β-Actin antibody was used as the loading control. Western blotting membrane results are shown in Figure 3.8.

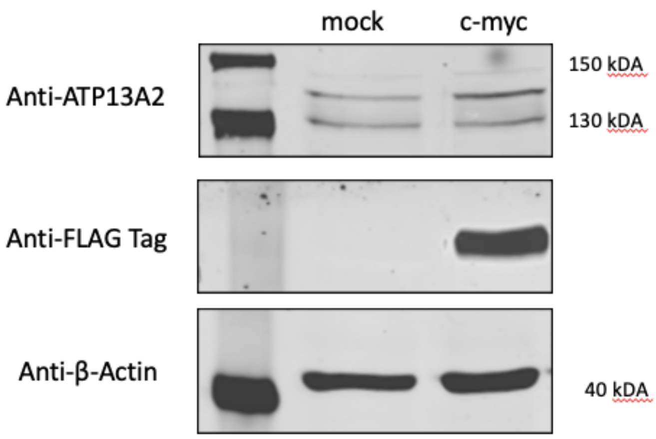

Figure 3.8: The level of ATP13A2 compared to control cell lysate and c-Myc overexpressed cell lysate. First lane shows the pre-stained protein ladder. Second lane shows the mock cell lysate. Third lane shows the c-Myc overexpressed cell lysate.

Statistically analyzed expression of the western blot protein levels are shown in Figure 3.9. The protein band intensities were measured by using the Li-Cor Biosciences Image Studio Software. ATP13A2 protein expression levels were normalized by the β-Actin protein expression levels in order to normalize each lane within itself.

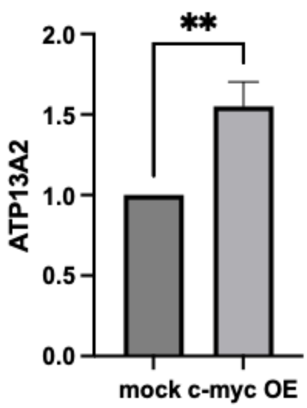

Figure 3.9: The histogram of normalized ATP13A2 protein expression levels on HEK293T cells.

Finally, the control lane and c-Myc overexpressed lane was normalized in order to detect the ATP1A3A2 protein expression fold change differences between two experimental conditions. These results indicated that when c-Myc transcription factor was overexpressed in HEK293T cells, ATP13A2 protein levels were significantly increased 1.5 folds compared to control, mock vector transfected group.

3.4.1 The effect of c-Myc transcription factor on HIF1α mRNA expression levels

Total RNA was isolated from mock and c-Myc overexpressed HEK293T cells to be turned into cDNA for qRT-PCR experiments. The experiment was done twice with duplicates. The fold changes of all of the collective experiments are given in Figure 3.10.

All of the results were statistically analyzed with t-test using GraphPad Prism software. qRT-PCR results showed that when c-Myc transcription factor was overexpressed in HEK293T cells, 48 hours after the c-Myc transfection, 1.5-fold increase was observed in HIF1α mRNA expression levels.

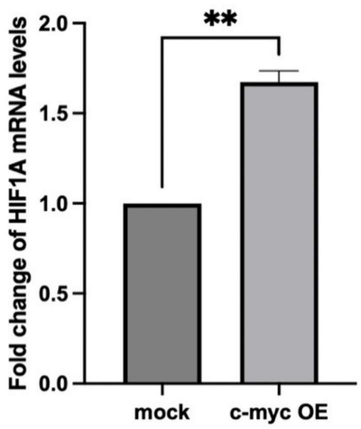

Figure 3.10: Fold change of HIF1α mRNA levels, 48 hours after c-Myc transcription factor overexpression.

3.4.2 The effect of c-Myc transcription factor on HIF1α protein expression levels

For the western blot experiments, the total proteins from control and c-Myc transfected HEK293T cells were isolated, 40-46 hours after the transfection of c-Myc transcription factor. Total proteins from KRS patient fibroblasts were also isolated 40-46 hours after fibroblasts were transfected with c-Myc using Amaxa® Cell Line Nucleofector® in order to detect changes in HIF1α protein expression based on increased c-Myc levels.

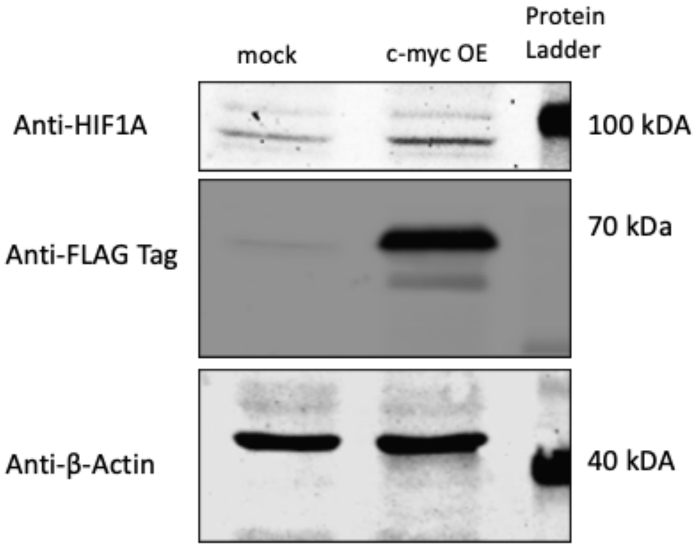

Figure 3.11: The level of HIF1α compared to control cell lysate and c-Myc overexpressed cell lysate in HEK293T cells. First lane shows the mock cell lysate. Second lane shows the c-Myc overexpressed cell lysate. Third lane shows the pre-stained protein ladder.

Once the FLAG-expression was detected in c-Myc transfected cells, the membranes were incubated in HIF1α antibody for 48 hours. β-Actin was used as the loading control. Western blotting results are shown in Figure 3.11.

Statistically analysed HIF1α expression levels on c-Myc overexpressed HEK293T cells and c-Myc overexpressed KRS patient fibroblasts are shown in Figure 3.12 and 3.13 respectively. These results indicated that when c-Myc was overexpressed in HEK293T cells and patient fibroblasts, HIF1α protein levels were significantly increased compared to control (mock) group which was expected based on the information found in the literature.

HIF1α protein calculated molecular weight is reported to be 93 kDa however it can be observed at 120 kDa due to post-translational modifications (Wang et al.,1995).

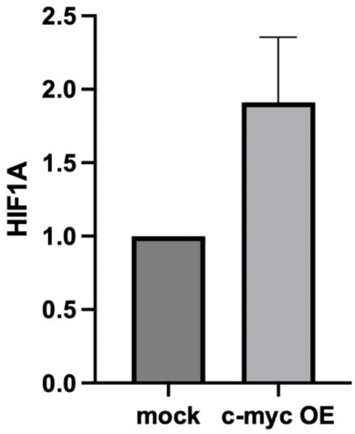

Figure 3.12: The histogram of normalized HIF1α protein expression in HEK293T cells.

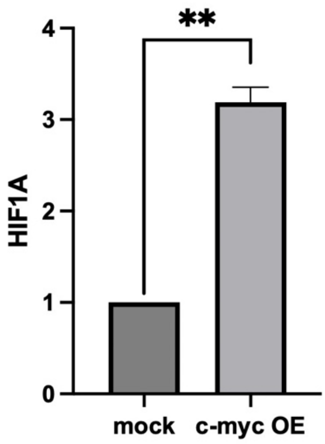

Figure 3.13: The histogram of normalized HIF1α protein expression in KRS patient fibroblasts.

3.4.3 Measuring the effects of c-Myc transcription factor on the ATP13A2 protein expression levels at certain time-points.

In order to investigate the underlying mechanism of contradictory decreasing mRNA levels and increasing protein levels, experiments were set up to detect initial short-term and long-term changes in the expression levels of ATP13A2 upon c-Myc overexpression. C-Myc transfected HEK293T cell were collected in a timely manner. After the c-Myc transfection, cell pellets were collected at 6th, 7th, 8th, 24th and 50th hour for western blotting and qRT-PCR experiments. For western blot experiments, once the FLAG-expression was detected in c-Myc transfected cells, the membranes were incubated in ATP13A2 antibody for 48 hours. β-Actin was used as the loading control. Western blot images are shown in Figure 3.14. Analyzed western blot results are shown in Figure 3.15.

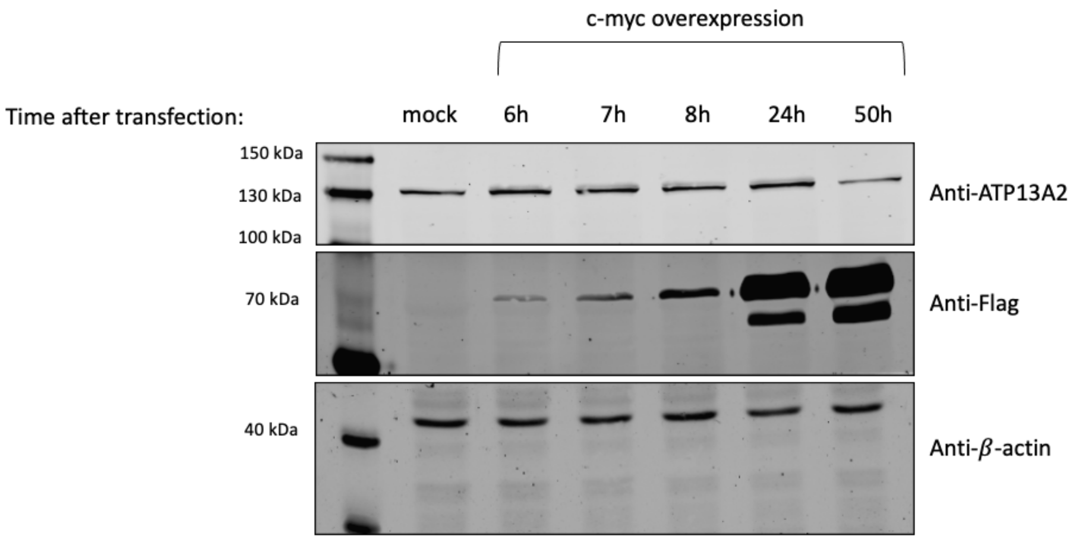

Figure 3.14: The ATP13A2 protein level comparison between HEK293T cell lysates collected at different time points after the transfection of 3X-FLAG-CMV-10 plasmid containing the *c-Myc* gene.

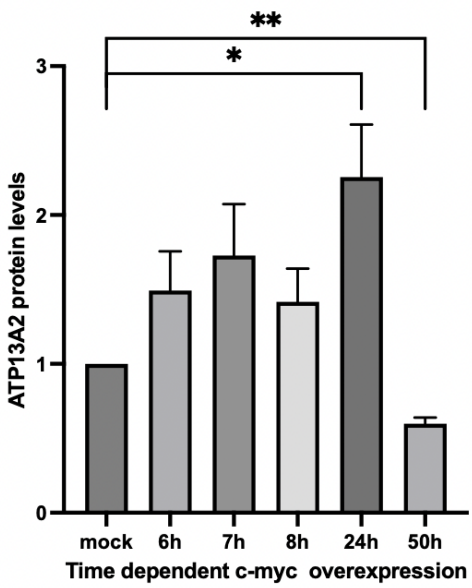

Figure 3.15: The histogram of normalized ATP13A2 protein expression levels on c-Myc overexpressed HEK293T cells collected at different time points.

The results showed that 6 hours after the transfection process, overexpressed c-Myc transcription factor could be observed faintly by using the FLAG antibody. The initial upregulating effects of c-Myc transcription factor on the expression levels of *ATP13A2* gene was observed around the 7th hour. Then, a slight decrease in the ATP13A2 protein expression was observed between the 7th and 8th hour. 24 hours after the transfection of *c-Myc* gene, the ATP13A2 protein levels were significantly increased however, approximately 50 hours after c-Myc transfection, ATP13A2 protein level was significantly downregulated compared to 24 hours after the c-Myc transfection.

3.4.4 Measuring the effects of c-Myc transcription factor on the ATP13A2 mRNA expression levels over time.

Total RNA was isolated from c-Myc transfected HEK293T cells. The cells were collected at 6^{th}, 7^{th}, 8^{th}, 24^{th} and 50^{th} hour after the c-Myc transfection. The fold changes of all of the collective experiments are given in Figure 3.16. Analyzed results showed that compared to the control group, ATP13A2 mRNA levels initially increased around 7^{th} and 8^{th} hours after c-Myc transfection. 24 hours after c-Myc transfection, ATP13A2 mRNA levels significantly increased however, approximately 50 hours after the c-Myc transfection process, the mRNA levels of ATP13A2 seem to be decreased compared to the control "mock" group.

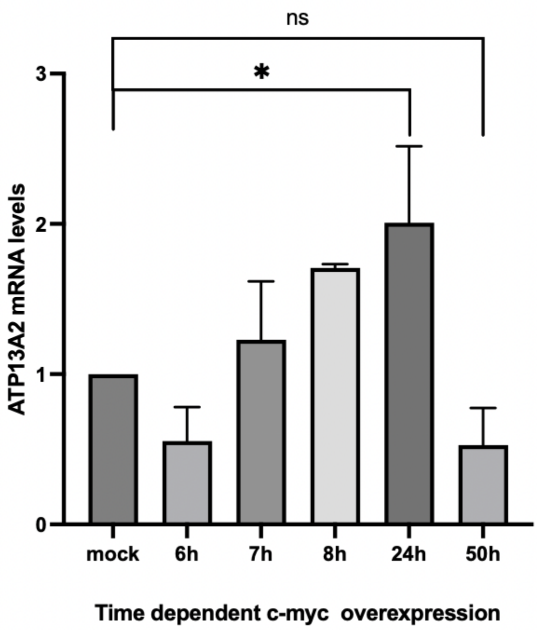

Figure 3.16: Fold changes of ATP13A2 mRNA levels upon c-Myc overexpression at certain time points.

3.5 Determination of the Truncated ATP13A2 Protein After c-Myc Overexpression on Homozygous Frameshift Mutated Patient Fibroblasts.

Previously, research done in our laboratory has shown that homozygous mutation c.1422_1423del:p.P474fs in the *ATP13A2* gene that we described earlier causes a pre-termination codon (PTC) and that the expression of mutant ATP13A2 mRNA is degraded by the mechanism of nonsense-mediated decay, inhibits the expression of ATP13A2 protein in patients' fibroblasts (Kırımtay et al. 2020).

In order to determine the direct effects of c-Myc in patient fibroblasts, c-Myc transcription factor was overexpressed in patient fibroblasts using the Amaxa Nucleofector device. Control group for the western blot experiment was untreated patient fibroblasts, carrying the same homozygous frameshift mutation that results with a pre-termination codon (PTC). The experiments results show that when patient fibroblast cells were transfected with c-Myc transcription factor, truncated mutant ATP13A2 protein was detected at 50 kDa, as expected (Figure 3.17).

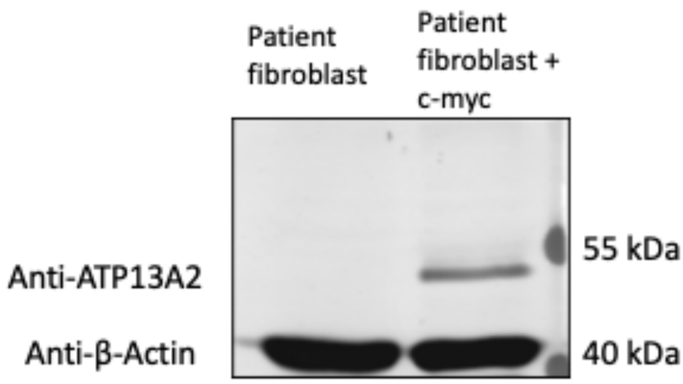

Figure 3.17: Mutant ATP13A2 protein detected on c-Myc overexpressed patient fibroblasts.

4. DISCUSSION AND CONCLUSION

The initial study performed in our laboratory using the 5-azacytidine treatment for NMD inhibition, an increase in ATP13A2 mRNA levels in control fibroblasts was observed. Since western blot results showed an increase in c-Myc protein levels, along with supporting bioinformatics research, it was hypothesized that c-Myc could have an increasing effect on ATP13A2 protein and mRNA levels.

However, c-Myc mRNA was identified as an NMD target in the literature, meaning that *c-Myc* is one of the genes that are normally regulated by the NMD mechanism within the cell (Li et al., 2015). Due to c-Myc proto-oncogene's ability of influencing major cellular functions and hundreds of target genes, in normal cellular circumstances, c-Myc mRNA and protein levels are tightly controlled by the NMD mechanism, causing c-Myc mRNA to degrade rapidly (Dang, 2012). 5-azacytidine treatment increasing intracellular c-Myc levels due to inhibiting its degradation, is expected. Considering the information in the literature, 5-azacytidine treatment increasing both ATP13A2 and c-Myc protein levels might not be sufficient enough on its own to prove that c-Myc transcription factor was the direct reason why ATP13A2 mRNA levels increased in healthy fibroblasts after 5-azacytidine administration.

However, according to our bioinformatics analysis, it was found that c-Myc transcription factor had several different binding sites present at *ATP13A2* promoter region. In order to confirm the potential binding sites in vivo, ChIP assay was performed. ChIP assay showed significant binding at the highest scored binding site labelled as F1/R1, that targeted the E-box variant located at -978 bp upstream of *ATP13A2* promoter region which supported the hypothesis of c-Myc transcription factor interacting and regulating the expression levels of *ATP13A2* gene.

To determine the effects of *c-Myc* proto-oncogene's direct effect on ATP13A2 mRNA levels, qRT-PCR experiments were done. The results indicated that when c-Myc transcription factor was overexpressed in HEK293T cells, ATP13A2 mRNA levels decreased significantly after 40-46 hours. To validate these results luciferase assay was also done to determine the c-Myc's effects on the promoter region directly. Luciferase assay also showed that when c-Myc was overexpressed on HEK293T cells, 40-46 hours after the transfection, the ATP13A2 expression was decreased significantly. Interestingly, when c-Myc was overexpressed in HEK293T cells and total protein was isolated from these cells 40-46 hours afterwards, western blot experiments showed a significant 1.5-fold increase in ATP13A2 protein levels. There might be several different reasons why c-Myc seems to decrease the mRNA levels but increase the ATP13A2 protein levels.

Firstly, the *c-Myc* gene has a significant impact on cellular metabolism. Since it has such drastic effects on the major cellular pathways, when the c-Myc regulation is derailed, it can lead to different types of cancer depending on the cell type. The *c-Myc* oncogene is found to be overexpressed in the majority of human carcinomas and is responsible for at least 40 percent of tumors (Dang, 2009).

An interesting fact is that since c-Myc binding sequence is not extremely specific, multiple studies indicate that Myc can bind to thousands of genes however only a small amount of these genes can actually respond directly to Myc only. c-Myc mediated transcriptional activity often involves other transcriptional factors participation (Dang et al.,2009). It is also reported that amplification of RNA is a distinct and functionally unrelated effect of Myc overexpression, as opposed to the upregulation of each active gene in a direct manner. RNA amplification is an indirect consequence of Myc, which functions mainly by means of differential regulation of particular sets of genes. This could suggest that the binding partners of c-Myc to the *ATP13A2* promoter region must be further investigated to reveal if c-Myc binds with its activator or repressor transcription partners.

Based on the results we obtained, it can be hypothesized that the c-Myc transcription factor's effect changes drastically depending on the duration it is present in the cellular environment. Even when it is initially expressed at low levels, due to its indirect consequence of RNA amplification, it seems to have an increasing effect of the ATP13A2 expression levels. To detect short-term and long-term effects, cell pellets were collected at certain time points (6^{th}, 7^{th}, 8^{th}, 24^{th} and 50^{th} hour) after c-Myc transfection. As c-Myc levels and its residence time inside the cell increases, it seems to have a downregulating effect on ATP13A2 mRNA and protein levels. 24 hours after the c-Myc transfection, the protein and mRNA levels of ATP13A2 found to be increased significantly however when 48-50 hours pass after c-Myc transfection, both the mRNA and protein levels were found to be downregulated.

There might be several reasons on why increased c-Myc levels cause a fluctuation in ATP13A2 expression levels.

Firstly, c-Myc transcription factor might be directly downregulating *ATP13A2* gene but it might be observed later than expected due the c-Myc transcription factor's indirect effects of increased RNA amplification. It has been demonstrated that c-Myc transcription factor inhibits the expression of H-ferritin, the heavy subunit of the protein ferritin responsible for storing intracellular iron. The regulation of H-ferritin and IRP2 by c-Myc may result in complementary effects that contribute to the intracellular iron reservoirs (Wu et al., 1999). ATP13A2 is one of the principal P-type ATPase family members. Liu et al. (2013) and Chung et al. (2019) report that ATP13A2 has the similar ion pump function like the majority of its family members. Importantly, it can also regulate the autophagy process. In KRS patients with homozygous mutant *ATP13A2* genes, the absence of wild-type ATP13A2 protein gives rise to iron accumulation within the cells. c-Myc also functions as a transcriptional activator of iron import genes TfR1 and DMT1 and represses ferritin expression in order to augment the intracellular labile iron pool (LIP) when intracellular iron levels are low (Brown et al., 2020). Another important point is that cancer cells are reported to be more dependent on iron compared to healthy cells (Chen et al., 2019). C-Myc, being one of the most important oncogenes, might simply try to increase the intracellular iron levels by increasing iron importing proteins and decreasing iron pumps.

Another reason might be that c-Myc is known for being a master transcriptional regulator and effecting the expression of a wide set of genes within the cells. In the light of the information known in the literature about HIF1α transcription factor upregulating ATP13A2 protein expression, changes in HIF1α expression levels were targeted for analysis upon c-Myc overexpression, in order to clarify if c-Myc transcription factor might have had an indirect effect on ATP13A2 protein expression via upregulating HIF1α transcription factor. In this case, the direct binding of c-Myc might be responsible for the decreasing ATP13A2 mRNA while it's indirect effects of increasing and stabilizing cellular HIF1α expression, might compensate for the decreased mRNA ATP13A2 expression and even lead to increased ATP13A2 protein expression for a certain amount of time. HIF1α is also known as a master regulator where it is meant to program the entirety of the cell to survive under hypoxic conditions. Hypoxia-inducible factors (HIFs) have been observed to exert influences on several aspects of tumor biology, including the immune evasion mechanisms employed by tumors, the invasiveness of cancer cells, the ability of tumors to spread to distant sites (metastasis), and their resistance to chemotherapy. In the case of HIF1α controlling ATP13A2 expression levels, reasoning is thought to depend on the iron homeostasis pathway as well. HIF1α transcription factor is known to regulate the expression of neuroprotective genes involved in cellular stress responses, which *ATP13A2* can also be considered under these terms.

Based on the results of our experiments that were conducted in a timely manner, it can be hypothesized that initially, when c-Myc transcription factor is overexpressed, both mRNA and protein levels of *ATP13A2* gene were found to be increased around 7^{th} and 8^{th} hour however, 50 hours after the c-Myc transfection, ATP13A2 mRNA levels were found to be significantly decreased. These results might also be the indication that the initial increase in the ATP13A2 expression levels might induce a feedback signal and later on, decrease the mRNA and protein levels of ATP13A2, despite the fact that c-Myc transcription factor is still highly overexpressed.

Furthermore, when the c-Myc was overexpressed in HEK293T cells and KRS patient fibroblasts, a known ATP13A2 upregulating transcription factor HIF1α was also found increased in both mRNA and protein expression levels. As mentioned above, due the c-Myc transcription factor's nature of interacting with many different binding partners for stable binding and controlling the expression levels of many different sets of genes, overall makes it very difficult to pinpoint a certain protein increase directly only to c-Myc transcription factor.

Finally, when patient fibroblasts were transfected with c-Myc, truncated mutant ATP13A2 protein was detected at 50 kDa compared to the non-transfected patient fibroblasts which did not express the mutant ATP13A2 since the mRNA is degraded by the mechanism of non-sense mediated decay. These results indicate that when c-Myc was overexpressed, the NMD mechanism was inhibited and the truncated protein was expressed. These findings are also supported by the literature information stating that NMD is inhibited by high Myc expression (Wang et al.,2011).

In conclusion, additional experiments should be carried out to identify potential transcription factor partners for c-Myc partners. Identifying the binding of c-Myc to the *ATP13A2* promoter region might not be enough on its own to confidently comment on its direct effect thus, the identification of binding partners of c-Myc to *ATP13A2* promoter region at that instant could be crucial to be certain of c-Myc transcription factor's direct effect on ATP13A2 expression. Cloning and co-transfecting some of the c-Myc binding partners alongside with c-Myc in order to repeat the luciferase assay in a time dependent manner might also uncover some of the uncertainty on the matter.

Also, conducting more time-dependent experiments by targeting the ATP13A2 mRNA and protein levels with even more frequent intervals could further enlighten the direct effects of c-Myc transcription factor.

REFERENCES

Brown, R. A. M., Richardson, K. L., Kabir, T. D., Trinder, D., Ganss, R., & Leedman, P. J. (2020). Altered Iron Metabolism and Impact in Cancer Biology, Metastasis, and Immunology. In Frontiers in Oncology (Vol. 10). Frontiers Media S.A. https://doi.org/10.3389/fonc.2020.00476

Bustamante-Barrientos, F. A., Méndez-Ruette, M., Ortloff, A., Luz-Crawford, P., Rivera, F. J., Figueroa, C. D., Molina, L., & Bátiz, L. F. (2021). The Impact of Estrogen and Estrogen-Like Molecules in Neurogenesis and Neurodegeneration: Beneficial or Harmful? In Frontiers in Cellular Neuroscience (Vol. 15). Frontiers Media S.A. https://doi.org/10.3389/fncel.2021.636176

Carroll, P. A., Freie, B. W., Mathsyaraja, H., & Eisenman, R. N. (2018). The MYC transcription factor network: balancing metabolism, proliferation and oncogenesis. In Frontiers of Medicine (Vol. 12, Issue 4, pp. 412–425). Higher Education Press. https://doi.org/10.1007/s11684-018-0650-z

Chen, X., Zhou, M., Zhang, S., Yin, J., Zhang, P., Xuan, X., Wang, P., Liu, Z., Zhou, B., & Yang, M. (2021). Cryo-EM structures and transport mechanism of human P5B type ATPase ATP13A2. Cell Discovery, 7(1). https://doi.org/10.1038/s41421-021-00334-6

Chen, Y., Fan, Z., Yang, Y., & Gu, C. (2019). Iron metabolism and its contribution to cancer (Review). In International Journal of Oncology (Vol. 54, Issue 4, pp. 1143–1154). Spandidos Publications. https://doi.org/10.3892/ijo.2019.4720

Dang, C. v. (2012). MYC on the path to cancer. In Cell (Vol. 149, Issue 1, pp. 22–35). Elsevier B.V. https://doi.org/10.1016/j.cell.2012.03.003

Dang, C. v., Le, A., & Gao, P. (2009). MYC-induced cancer cell energy metabolism and therapeutic opportunities. Clinical Cancer Research, 15(21), 6479–6483. https://doi.org/10.1158/1078-0432.CCR-09-0889

Dang, T., Cao, W. J., Zhao, R., Lu, M., Hu, G., & Qiao, C. (2022). ATP13A2 protects dopaminergic neurons in Parkinson's disease: from biology to pathology. Journal of Biomedical Research, 36(2), 98–108. https://doi.org/10.7555/JBR.36.20220001

Gitler, A. D., Chesi, A., Geddie, M. L., Strathearn, K. E., Hamamichi, S., Hill, K. J., Caldwell, K. A., Caldwell, G. A., Cooper, A. A., Rochet, J. C., & Lindquist, S. (2009). α-Synuclein is part of a diverse and highly conserved interaction network that includes PARK9 and manganese toxicity. Nature Genetics, 41(3), 308–315. https://doi.org/10.1038/ng.300

Graham, F. L., Smileyt, J., Russell, W. C., & Nairn, R. (1977). Characteristics of a Human Cell Line Transformed by DNA from Human Adenovirus Type 5. In J. gen. Virol (Vol. 36).

Karousis, E. D., Nasif, S., & Mühlemann, O. (2016). Nonsense-mediated mRNA decay: novel mechanistic insights and biological impact. Wiley Interdisciplinary Reviews: RNA, 7(5), 661–682. https://doi.org/10.1002/wrna.1357

Kong, S. M. Y., Chan, B. K. K., Park, J. S., Hill, K. J., Aitken, J. B., Cottle, L., Farghaian, H., Cole, A. R., Lay, P. A., Sue, C. M., & Cooper, A. A. (2014). Parkinson's disease-linked human PARK9/ATP13A2 maintains zinc homeostasis and promotes α-Synuclein externalization via exosomes. Human Molecular Genetics, 23(11), 2816–2833. https://doi.org/10.1093/hmg/ddu099

Li, T., Shi, Y., Wang, P., Guachalla, L. M., Sun, B., Joerss, T., Chen, Y., Groth, M., Krueger, A., Platzer, M., Yang, Y., Rudolph, K. L., & Wang, Z. (2015). Smg6/Est1 licenses embryonic stem cell differentiation via nonsense-mediated mRNA decay . The EMBO Journal, 34(12), 1630–1647. https://doi.org/10.15252/embj.201489947

Lin, C. Y., Lovén, J., Rahl, P. B., Paranal, R. M., Burge, C. B., Bradner, J. E., Lee, T. I., & Young, R. A. (2012). Transcriptional amplification in tumor cells with elevated c-Myc. Cell, 151(1), 56–67. https://doi.org/10.1016/j.cell.2012.08.026

Mufudza, C., Sorofa, W., & Chiyaka, E. T. (2012). Assessing the effects of estrogen on the dynamics of breast cancer. Computational and Mathematical Methods in Medicine, 2012. https://doi.org/10.1155/2012/473572

Nasif, S., Contu, L., & Mühlemann, O. (2018). Beyond quality control: The role of nonsense-mediated mRNA decay (NMD) in regulating gene expression. In Seminars in Cell and Developmental Biology (Vol. 75, pp. 78–87). Elsevier Ltd. https://doi.org/10.1016/j.semcdb.2017.08.053

Noch E, Henchcliffe C, Hellmers N, Chu ML, Pappas J, Moran E, Alcaraz W, Sarva H. (2017). Kufor-Rakeb Syndrome Due to a Novel ATP13A2 Mutation in 2 Chinese-American Brothers. Mov Disord Clin Pract. 2017 Dec 21;5(1):92-95. doi: 10.1002/mdc3.12567. PMID: 30746398; PMCID: PMC6336435.

Rajagopalan S, Rane A, Chinta SJ, Andersen JK. Regulation of ATP13A2 via PHD2-HIF1α Signaling Is Critical for Cellular Iron Homeostasis: Implications for Parkinson's Disease. J Neurosci. (2016). Jan 27;36(4):1086-95. doi: 10.1523/JNEUROSCI.3117-15.2016. PMID: 26818499; PMCID: PMC6404282.

Ramirez, A., Heimbach, A., Gründemann, J., Stiller, B., Hampshire, D., Cid, L. P., Goebel, I., Mubaidin, A. F., Wriekat, A. L., Roeper, J., Al-Din, A., Hillmer, A. M., Karsak, M., Liss, B., Woods, C. G., Behrens, M. I., & Kubisch, C. (2006). Hereditary parkinsonism with dementia is caused by mutations in ATP13A2, encoding a lysosomal type 5 P-type ATPase. Nature Genetics, 38(10), 1184–1191. https://doi.org/10.1038/ng1884

Siddiq A, Ayoub IA, Chavez JC, Aminova L, Shah S, LaManna JC, Patton SM, Connor JR, Cherny RA, Volitakis I, Bush AI, Langsetmo I, Seeley T, Gunzler V, Ratan RR. Hypoxia-inducible factor prolyl 4-hydroxylase inhibition: A target for neuroprotection in the central nervous system. J Biol Chem. 2005;280:41732–41743.

Thomas, P., & Smart, T. G. (2005). HEK293 cell line: A vehicle for the expression of recombinant proteins. Journal of Pharmacological and Toxicological Methods, 51(3), 187–200. https://doi.org/10.1016/J.VASCN.2004.08.014

van Veen, S., Sørensen, D. M., Holemans, T., Holen, H. W., Palmgren, M. G., & Vangheluwe, P. (2014). Cellular function and pathological role of ATP13A2 and related P-type transport ATPases in Parkinson's disease and other neurological disorders. In Frontiers in Molecular Neuroscience (Vol. 7, Issue MAY). Frontiers Research Foundation. https://doi.org/10.3389/fnmol.2014.00048

Vegeto, E., Villa, A., della Torre, S., Crippa, V., Rusmini, P., Cristofani, R., Galbiati, M., Maggi, A., & Poletti, A. (2019). The role of sex and sex hormones in neurodegenerative diseases. In Endocrine Reviews (Vol. 41, Issue 2). Endocrine Society. https://doi.org/10.1210/endrev/bnz005

Wang JY, Zhuang QQ, Zhu LB, Zhu H, Li T, Li R, Chen SF, Huang CP, Zhang X, Zhu JH. Meta-analysis of brain iron levels of Parkinson's disease patients determined by postmortem and MRI measurements. Sci Rep. (2016) Nov 9; 6:36669. doi: 10.1038/srep36669. PMID: 27827408; PMCID: PMC5101491.

Wang, D., Wengrods, J., & Gardners, L. B. (2011). Overexpression of the c-myc oncogene inhibits nonsense-mediated RNA decay in B lymphocytes. Journal of Biological Chemistry, 286(46), 40038–40043. https://doi.org/10.1074/jbc.M111.266361

Wang, G. L., & Semenza, G. L. (1995). Purification and characterization of hypoxia-inducible factor. Journal of Biological Chemistry, 270(3), 1230–1237. https://doi.org/10.1074/jbc.270.3.1230

Wu KJ, Polack A, Dalla-Favera R. (1999). Coordinated regulation of iron-controlling genes, H-ferritin and IRP2, by c-MYC. Science. Jan 29;283(5402):676-9. doi: 10.1126/science.283.5402.676. PMID: 9924025.

Xu Q, Guo H, Zhang X, Tang B, Cai F, Zhou W, Song W. Hypoxia regulation of ATP13A2 (PARK9) gene transcription. J Neurochem. (2012); 122:251–259. doi: 10.1111/j.1471-4159.2012.07676. x.

Yang X, Xu Y. Mutations in the ATP13A2 gene and Parkinsonism: a preliminary review. Biomed Res Int. (2014); 2014:371256. doi: 10.1155/2014/371256. Epub 2014 Aug 14. PMID: 25197640; PMCID: PMC4147200.

APPENDICES

Appendix A

Cloned *c-Myc* gene sequence is aligned with the reference *c-Myc* gene given down below for reference. In the cloned c-Myc sequence, N-terminal FLAG-tag that was also sequenced is shown in red letters. Reference *c-Myc* gene starts from the blue sequence.

```
CLUSTAL O(1.2.4) multiple sequence alignment


c-myc          ACCATGGACTACAAAGACCATGACGGTGATTATAAAGATCATGACATCGATTACAAGGAT 60
reference      ------------------------------------------------------------ 0


c-myc         GACGATGACAAGCTTGCGGCCGCGAATTCACTGGATTTTTTTCGGGTAGTGGAAAACCAG 120
reference     ------------------------------CTGGATTTTTTTCGGGTAGTGGAAAACCAG 27
                                            ******************************

c-myc         CAGCCTCCCGCGACGATGCCCCTCAACGTTAGCTTCACCAACAGGAACTATGACCTCGAC 180
reference     CAGCCTCCCGCGACGATGCCCCTCAACGTTAGCTTCACCAACAGGAACTATGACCTCGAC 87
              ************************************************************

c-myc         TACGACTCGGTGCAGCCGTATTTCTACTGCGACGAGGAGGAGAACTTCTACCAGCAGCAG 240
reference     TACGACTCGGTGCAGCCGTATTTCTACTGCGACGAGGAGGAGAACTTCTACCAGCAGCAG 147
              ************************************************************

c-myc         CAGCAGAGCGAGCTGCAGCCCCCGGCGCCCAGCGAGGATATCTGGAAGAAATTCGAGCTG 300
reference     CAGCAGAGCGAGCTGCAGCCCCCGGCGCCCAGCGAGGATATCTGGAAGAAATTCGAGCTG 207
              ************************************************************

c-myc         CTGCCCACCCCGCCCCTGTCCCCTAGCCGCCGCTCCGGGCTCTGCTCGCCCTCCTACGTT 360
reference     CTGCCCACCCCGCCCCTGTCCCCTAGCCGCCGCTCCGGGCTCTGCTCGCCCTCCTACGTT 267
              ************************************************************

c-myc         GCGGTCACACCCTTCTCCCTTCGGGGAGACAACGACGGCGGTGGCGGGAGCTTCTCCACG 420
reference     GCGGTCACACCCTTCTCCCTTCGGGGAGACAACGACGGCGGTGGCGGGAGCTTCTCCACG 327
              ************************************************************

c-myc         GCCGACCAGCTGGAGATGGTGACCGAGCTGCTGGGAGGAGACATGGTGAACCAGAGTTTC 480
reference     GCCGACCAGCTGGAGATGGTGACCGAGCTGCTGGGAGGAGACATGGTGAACCAGAGTTTC 387
              ************************************************************

c-myc         ATCTGCGACCCGGACGACGAGACCTTCATCAAAAACATCATCATCCAGGACTGTATGTGG 540
reference     ATCTGCGACCCGGACGACGAGACCTTCATCAAAAACATCATCATCCAGGACTGTATGTGG 447
              ************************************************************

c-myc         AGCGGCTTCTCGGCCGCCGCCAAGCTCGTCTCAGAGAAGCTGGCCTCCTACCAGGCTGCG 600
reference     AGCGGCTTCTCGGCCGCCGCCAAGCTCGTCTCAGAGAAGCTGGCCTCCTACCAGGCTGCG 507
              ************************************************************

c-myc         CGCAAAGACAGCGGCAGCCCGAACCCCGCCCGCGGCCACAGCGTCTGCTCCACCTCCAGC 660
reference     CGCAAAGACAGCGGCAGCCCGAACCCCGCCCGCGGCCACAGCGTCTGCTCCACCTCCAGC 567
              ************************************************************

c-myc         TTGTACCTGCAGGATCTGAGCGCCGCCGCCTCAGAGTGCATCGACCCCTCGGTGGTCTTC 720
reference     TTGTACCTGCAGGATCTGAGCGCCGCCGCCTCAGAGTGCATCGACCCCTCGGTGGTCTTC 627
              ************************************************************

c-myc         CCCTACCCTCTCAACGACAGCAGCTCGCCCAAGTCCTGCGCCTCGCAAGACTCCAGCGCC 780
reference     CCCTACCCTCTCAACGACAGCAGCTCGCCCAAGTCCTGCGCCTCGCAAGACTCCAGCGCC 687
              ************************************************************
```

```
c-myc       TTCTCTCCGTCCTCGGATTCTCTGCTCTCCTCGACGGAGTCCTCCCCGCAGGGCAGCCCC 840
reference   TTCTCTCCGTCCTCGGATTCTCTGCTCTCCTCGACGGAGTCCTCCCCGCAGGGCAGCCCC 747
            ************************************************************

c-myc       GAGCCCCTGGTGCTCCATGAGGAGACACCGCCCACCACCAGCAGCGACTCTGAGGAGGAA 900
reference   GAGCCCCTGGTGCTCCATGAGGAGACACCGCCCACCACCAGCAGCGACTCTGAGGAGGAA 807
            ************************************************************

c-myc       CAAGAAGATGAGGAAGAAATCGATGTTGTTTCTGTGGAAAAGAGGCAGGCTCCTGGCAAA 960
reference   CAAGAAGATGAGGAAGAAATCGATGTTGTTTCTGTGGAAAAGAGGCAGGCTCCTGGCAAA 867
            ************************************************************

c-myc       AGGTCAGAGTCTGGATCACCTTCTGCTGGAGGCCACAGCAAACCTCCTCACAGCCCACTG 1020
reference   AGGTCAGAGTCTGGATCACCTTCTGCTGGAGGCCACAGCAAACCTCCTCACAGCCCACTG 927
            ************************************************************

c-myc       GTCCTCAAGAGGTGCCACGTCTCCACACATCAGCACAACTACGCAGCGCCTCCCTCCACT 1080
reference   GTCCTCAAGAGGTGCCACGTCTCCACACATCAGCACAACTACGCAGCGCCTCCCTCCACT 987
            ************************************************************

c-myc       CGGAAGGACTATCCTGCTGCCAAGAGGGTCAAGTTGGACAGTGTCAGAGTCCTGAGACAG 1140
reference   CGGAAGGACTATCCTGCTGCCAAGAGGGTCAAGTTGGACAGTGTCAGAGTCCTGAGACAG 1047
            ************************************************************

c-myc       ATCAGCAACAACCGAAAATGCACCAGCCCCAGGTCCTCGGACACCGAGGAGAATGTCAAG 1200
reference   ATCAGCAACAACCGAAAATGCACCAGCCCCAGGTCCTCGGACACCGAGGAGAATGTCAAG 1107
            ************************************************************

c-myc       AGGCGAACACACAACGTCTTGGAGCGCCAGAGGAGGAACGAGCTAAAACGGAGCTTTTTT 1260
reference   AGGCGAACACACAACGTCTTGGAGCGCCAGAGGAGGAACGAGCTAAAACGGAGCTTTTTT 1167
            ************************************************************

c-myc       GCCCTGCGTGACCAGATCCCGGAGTTGGAAAACAATGAAAAGGCCCCCAAGGTAGTTATC 1320
reference   GCCCTGCGTGACCAGATCCCGGAGTTGGAAAACAATGAAAAGGCCCCCAAGGTAGTTATC 1227
            ************************************************************

c-myc       CTTAAAAAAGCCACAGCATACATCCTGTCCGTCCAAGCAGAGGAGCAAAAGCTCATTTCT 1380
reference   CTTAAAAAAGCCACAGCATACATCCTGTCCGTCCAAGCAGAGGAGCAAAAGCTCATTTCT 1287
            ************************************************************

c-myc       GAAGAGGACTTGTTGCGGAAACGACGAGAACAGTTGAAACACAAACTTGAACAGCTACGG 1440
reference   GAAGAGGACTTGTTGCGGAAACGACGAGAACAGTTGAAACACAAACTTGAACAGCTACGG 1347
            ************************************************************

c-myc       AACTCTTGTGCGTAAGGATCCCGGGTGGCATC        1472
reference   AACTCTTGTGCGTAA-----------------        1362
            ***************
```

Appendix B

Table B.1: Bioinformatic tools, the purpose of tools and their website URL.

Tool Name	Using Purpose	Website URL
Genome Browser, UCSC (University of California, Santa Cruz)	Acquiring sequences of the human *ATP13A2* promoter and 5'-UTR	http://ucscbrowser.genap.ca/
The National Center for Biotechnology Information (NCBI)	Acquiring human *c-Myc* coding sequence	https://www.ncbi.nlm.nih.gov/projects/CCDS/CcdsBrowse.cgi
MATCHTM public version 1.0, geneXplain	Determining possible c-Myc binding sites on ATP13A2 promoter sequence	http://gene-regulation.com/cgi-bin/pub/programs/match/bin/match.cgi
OligoAnalyzer 3.1, Integrated DNA Technologies (IDT)	In order to design primers while taking into account their Tm, GC content, and self-dimer formation	https://eu.idtdna.com/pages/tools/oligoanalyzer
Tm Calculator, New England BioLabs	To confirm the annealing temperatures of the primers	https://tmcalculator.neb.com/#!/main
TFBIND Web Software	To determine possible c-Myc binding sites on *ATP13A2* promoter sequence	https://tfbind.hgc.jp/

Table B.2: Instruments used during this study and the supplier company.

Instruments	Company
Sigma 6K15 Centrifuge	Beckman Coulter
SpectrafugeTM Mini Centrifuge	Labnet International
MiniCell® PrimoTM EC320 Electrophoretic Gel System	Thermo Electron
Microfuge®18 Centrifuge	Beckman Coulter
Finnpipette Electronic Pipette	Thermo Scientific
Benchtop pH Meter	Mettler Toledo
-80°C Freezer	New Brunswixk Scientific
4°C – 20 °C Freezer	UĞUR
FormaTM Steri-CycleTM CO2 Incubators	Thermo Scientific
Benchmark Plus Microplate Spectrophotometer	Bio-Rad
10 µl, 100 µl, 200 µl, 1000 µl Micropipette	Eppendorf
Magnetic Stirrer	Isolab
Hemocytometer	FisherLab Scientific
2.5 µl Micropipette	Promega
Magnetic Separation Rack	Bio-Rad
Powerpack Basic Power Supply	Bio-Rad
Trans-Blot® TurboTM Transfer System	Bio-Rad
Trans-Blot® SD Semi-Dry Transfer Cell	Bio-Rad
Mini-PROTEAN Tetra Cell System	VWR
Heat-block	VWR
Rocking Platform Shaker	Stuart
SB3 Rotator	Electro-Mag
M96KP Waterbath	FASTER
BH-EN 2003 Class II Microbiological Safety Cabinet	Olympus
CK40-F200 Inverted Light Microscope	Invitrogen
Countess® Automated Cell Counter	Lonza
NucleofectorTM 2b Device	Bandelin
Sonicator	Precisa
LS 620 SCS Precision weigher	Precisa
BJ 610 C Weigher	Roche
LightCycler® 480 Instrument	Thermo Electron
Fluoroskan AscentTM FL Microplate Flurometer and Luminometer	LI-COR
Odyssey® CLx Infrared Imaging System	Bio-Rad
Amaxa® Cell Line Nucleofector®	Lonza

Table B.3: Equipment that are used during this study and the supplier company.

Equipment	Company
15 ml, 50 ml Falcon Tubes	Sarstedt
1.5 ml, 2 ml Eppendorf Tubes	Axygen
UltraCruz® Nitrocellulose Pure Transfer Membranes (0.22 µm)	Santa Cruz
Tissue Culture Flasks (25 cm2, 75 cm2)	Sarstedt
Tissue Culture Plate (6 well, 12 well, 24 well)	Sarstedt
Tissue Culture Dish (60 mm diameter)	TPP
Petri Plate (100 mm diameter)	Isolab
Cell Scraper	TPP
CountessTM Counting Chamber Slide	Invitrogen
LightCycler® 480 Multiwell Plates	Roche
5 ml, 10 ml, 25 ml serological pipette	Sarstedt

Table B.4: Commercially available buffers/solutions and the supplier company.

Buffers and Solutions	Company
6X DNA Loading Dye	New England Biolabs
Acrylamide-bis Solution (40%) (ready to use)	Merck Millipore
Agar (American Bacteriological Agar)	Conda,Pronadisa
Ammonium persulfate (APS)	Sigma-Aldrich
Ampicillin sodium salt	Sigma-Aldrich
Boric acid (≥99.5%)	Sigma
Bovine Serum Albumin (BSA)	Sigma-Aldrich
Chloroform	Merck Millipore
Color Prestained Protein Standard	New England Biolabs
cOmplete Tablets EASYpack (Protease Inhibitor Cocktail Tablets)	Roche
Coomassie Brilliant Blue	Sigma-Aldrich
DMEM High glucose (4.5 g/L) w/L-glutamine (1X)	Lonza
DMSO	Thermo Fischer Scientific
Ethanol (absolute, ≥99.8% (GC))	Sigma-Aldrich
Ethylenediaminetetraacetic acid (EDTA)	Merch Millipore
Glycine	Merck Millipore
Hydrochloric acid (HCl) (37%)	Merck Millipore
Low Range DNA Ladder, ready-to-use	Thermo Fischer Scientific
Methanol (for HPLC, ≥99.9%)	Sigma-Aldrich
Nonfat Dry Milk	Sigma-Aldrich
Polyethylenimine (PEI) (Linear, MW 25,000)	Cell Signaling Technology
RIPA lysis Buffer	Santa Cruz
Nuclease-free dH2O)	Polysciences
Agarose	Merck Millipore
Phosphate buffered saline (PBS) Tablets	Lonza
Paraformaldehyde	VWR Amresco Life Sciences
Penicillin-Streptomycin (10K/10K	Merck Millipore
Isopropanol (2-propanol)	Lonza
Fetal Bovine Serum (FBS)	Merck Millipore
Glycerol	Biowest
Sodium chloride (NaCl)	Fisher Scientific
Sodium dodecyl sulfate (SDS)	Merck Millipore
Sodium hydroxide (NaOH)	Merck Millipore
Tetramethylethylenediamine (TEMED)	Merck Millipore
Tris Base (Molecular Biology Grade)	Merck Millipore
Tris-acetate-EDTA (TAE) Buffer (50X)	Merck Millipore
Trypan Blue Stain (0.4%)	Bio-Rad
Trypsin/EDTA	Invitrogen
Tryptone	Lonza
Tween® 20	LabM, Neogen Company
Yeast Extract	Thermo Fischer Scientific

Appendix C

Table C.1: Lower (separating) gel buffer.

Content	Amount
Tris base	181.5 (1.5M)
dH_2O	Up to 1L

Table C.2: Upper (stacking) gel buffer.

Content	Amount
Tris base	60.5g (0.5M)
dH_2O	Up to 1L

Table C.3: Separation Gel (10%) (for 2 gels)

Content	Amount
Acrylamide (40%)	2.54 ml
Separating buffer (1.5 M Tris)	3 ml
SDS 10%	120 µl
APS 10%	120 µl
TEMED	12 µl
dH_2O	4.36 ml

Table C.4: Stacking Gel (5%) (for 2 gels)

Content	Amount
Acrylamide (40%)	540 µl
Separating buffer (0.5 M Tris)	500 µl
SDS 10%	40 µl
APS 10%	40 µl
TEMED	4 µl
dH_2O	2.92 ml

Table C.5: SDS-PAGE Running Buffer (10X)

Content	Amount
Tris-base ($C_4H_{11}NO_3$)	8.3 g
Glycine ($C_2H_5NO_2$)	144 g
SDS ($NaC_{12}H_{25}SO_4$)	10 g
dH_2O	up to 1 liter

Table C.6: Transfer Buffer (1X)

Content	Amount
Tris base ($C_4H_{11}NO_3$)	3 g
Glycine ($C_2H_5NO_2$)	14.4 g
dH_2O	up to 800 ml
Methanol	200 ml

Table: C.7: TBS (10X)

Content	Amount
Tris,base ($C_4H_{11}NO_3$)	24 g
Sodium chloride (NaCl)	88 g
dH_2O	up to 1 liter

Table C.8: TBS-T buffer (1X)

Content	Amount
10X TBS Solution	100 ml
Tween-20	0.1 ml
dH_2O	up to 1 liter

Table C.9: Blocking Solution (5%)

Content	Amount
Non-fat dry milk	2.5 g
TBS-T	50ml

Appendix D:

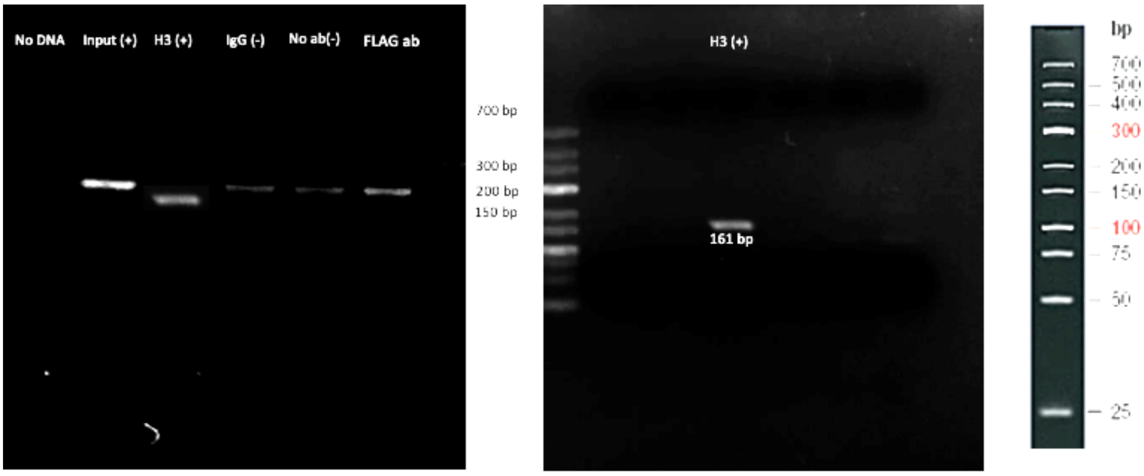

Figure D.1: PCR results of the investigation of c-Myc binding sites after ChIP assay. Potential positive binding at F3/R3 binding site and a non-determined faulty primer pair result at F4/R4 binding site respectively.

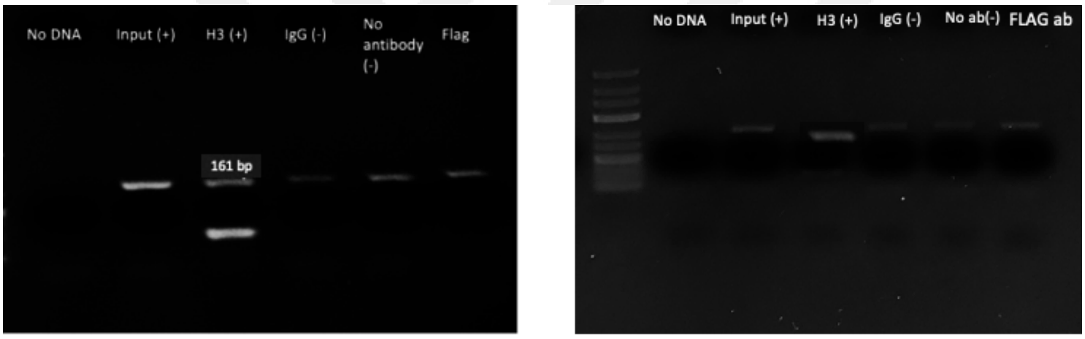

Figure D.2: PCR results of the investigation of c-Myc binding sites after ChIP assay. Negative binding at F5/R5 binding sites and potential positive binding at F6/R6 binding site respectively.

CURRICULUM VITAE

Name Surname : Aslı Beril Tiryakiler

Place and Date of Birth :

E-Mail :

EDUCATION :

- **B.Sc.** : Kadir Has University (2016-2020), Faculty of Engineering and Natural Sciences, Bioinformatics and Genetics Department (GPA: 3.92/4.00)

PROFESSIONAL EXPERIENCE AND REWARDS:

- Kadir Has University, Part-Time Lecturer (November 2020-)
- Izmir Biomedicine and Genome Center, Intern (July 2019 – August 2019)
- Oregon Health and Science University, Intern (June 2018 – September 2018)

PUBLICATIONS, PRESENTATIONS AND PATENTS ON THE THESIS:

- **Aslı Beril Tiryakiler**, Arzu Karabay**,** Investigation of Effects of c-Myc transcription factor on the expression level of *ATP13A2* gene (2023). *21st National Neuroscience Congress, 8-11 June 2023, Bolu, Turkey. (Poster presentation)*